Running Head: Tundra Response to Climate with Grazing

Model Responses to CO_2 and Warming Are Underestimated without Explicit Representation of Arctic Small-Mammal Grazing

Edward B. Rastetter[1,*], Kevin L. Griffin[2, 3, 4], Rebecca J. Rowe[5], Laura Gough[6], Jennie R. McLaren[7], and Natalie T. Boelman[4]

[1]The Ecosystems Center, Marine Biological Laboratory, Woods Hole, MA 02543, USA

[2]Department of Ecology, Evolution and Environmental Biology, Columbia University, New York, NY 10027, USA

[3]Department of Earth and Environmental Sciences, Columbia University, Palisades, NY 10964, USA

[4]Lamont-Doherty Earth Observatory, Columbia University, Palisades, NY 10964, USA

[5]Natural Resources and the Environment, University of New Hampshire, Durham, NH 03824, USA

[6]Department of Biological Sciences, Towson University, Towson, MD 21252, USA

[7] Department of Biological Sciences, University of Texas at El Paso, El Paso, TX 79968, USA

[*]Corresponding author, erastetter@mbl.edu

Open Research Statement: New empirical data were not used for this research. The code (Rastetter et al., 2021a) is available from Zenodo: http://doi.org/10.5281/zenodo.5083290 and the simulation results (Rastetter et al., 2021b & 2021c) are available from the Environmental Data Initiative: https://doi.org/10.6073/pasta/67108cef344d93cfdd060e7e0f0911f5 and https://doi.org/10.6073/pasta/42e6660b2d1f2b59985ed0940e53f0d4.

ABSTRACT

We use a simple model of coupled carbon and nitrogen cycles in terrestrial ecosystems to examine how explicitly representing grazers versus having grazer effects implicitly aggregated in with other biogeochemical processes in the model alters predicted responses to elevated carbon dioxide and warming. The aggregated approach can affect model predictions because grazer-mediated processes can respond differently to changes in climate from the processes with which they are typically aggregated. We use small-mammal grazers in arctic tundra as an example and find that the typical three-to-four-year cycling frequency is too fast for the effects of cycle peaks and troughs to be fully manifested in the ecosystem biogeochemistry. We conclude that implicitly aggregating the effects of small-mammal grazers with other processes results in an underestimation of ecosystem response to climate change relative to estimations in which the grazer effects are explicitly represented. The magnitude of this underestimation increases with grazer density. We therefore recommend that grazing effects be incorporated explicitly when applying models of ecosystem response to global change.

KEYWORDS: arctic tundra, biogeochemistry, carbon cycling, carbon-nitrogen ecosystem model, climate change, nitrogen cycling, population cycles, small-mammal herbivores

INTRODUCTION

Despite evidence that animals can influence ecosystem carbon (C) and nutrient cycles (Schmitz et al., 2014), explicit incorporation of animals into terrestrial biogeochemical models is rare (Metcalfe and Olofsson 2015). To maintain mass balance in these models without explicit representation of animals, the effects of animals have to be implicitly aggregated into other biochemical processes though model calibration (e.g., animal respiration included with other heterotrophic respiration). However, animal-mediated processes can behave differently from the processes with which they are aggregated. For example, combining microbial and mammal respiration into a single value for heterotrophic respiration can cause problems because warming generally increases respiration in microbes, but can slow respiration in mammals if the warming reduces the energy needed to maintain body temperature (Batzli et al., 1980). Here we examine the effects of aggregating grazer-mediated processes in with other biogeochemical processes when modeling ecosystem response to elevated carbon dioxide (CO_2) and warming. We use small-mammal grazers in arctic tundra as an example. However, the principles are general, and we conclude with a discussion of how our results might apply more generally to other grazers and other ecosystems.

Recent studies suggest that animals influence the response of tundra to climate change (Tuomi et al., 2019, Petit Bon et al., 2020). Experimental manipulations conducted across a range of tundra ecosystems have shown that while warming or fertilization typically enhances above ground productivity and nutrient cycling in tundra, the presence of herbivores - including rodents, geese, and ungulates - can dampen or negate this response (e.g., Grellman et al., 2002, Sjögersten et al., 2008, Post and Pedersen 2008, Rinnan et al., 2009, Cahoon et al., 2011, Kaarlejärvi et al., 2015, Leffler et al., 2019) or might enhance productivity (Gough et al., 2012).

64 Further, observational studies have shown that trophic interactions on the tundra strengthen
65 under warmer conditions (McKinnon et al., 2010, Legagneux et al., 2012), suggesting that
66 animal influences on arctic C cycling might be stronger in the future.
67 In other terrestrial ecosystems, animals are known to affect C and nutrient cycling
68 (McNaughton 1985, McLaren and Jefferies 2004, Wilkinson and Sherratt 2016). The direct
69 effects of animals vary among ecosystems, type of herbivore, and plant growth form (Jai et al.
70 2018) but have historically been thought of as small relative to plant and microbial processes
71 (e.g., Hairston et al., 1960). Nevertheless, animals can accelerate nutrient cycles and influence
72 plants and microbes indirectly by mediating chemical and biological processes and altering
73 community structure and can thereby have a large influence on ecosystem C and nutrient
74 processing (Pastor et al., 1988, Schmitz et al., 2014, Wardle et al., 2004, Zimov et al., 2009,
75 Metcalfe et al., 2014).
76 Although herbivore-vegetation models have been made for other ecosystems (e.g., Seagle
77 and McNaughton 1993, Bennett 2003), we are aware of only one vegetation-dynamics model -
78 ArcVeg - that explicitly addresses the effect of an arctic herbivore (caribou) on tundra
79 biogeochemistry (Yu et al., 2011). This model indicates that grazing dampens the increase in
80 plant biomass expected from warming soils and the consequent increase in nutrient cycling (Yu
81 et al., 2011). These results suggest that the explicit inclusion of grazers in biogeochemical
82 models could be necessary for predicting tundra responses to climate change.
83 Other modeling studies have addressed arctic biogeochemical responses to climate
84 change, but without the explicit representation of the effects of animals as separate from other C
85 and nutrient cycling processes. These biogeochemical models indicate significant long-term
86 impacts of elevated CO_2 and warming, but the model predictions differ on how these responses

87 will ultimately affect net C source versus sink activity. This source-sink disparity is due to
88 uncertainty in the balance between elevated autotrophic and heterotrophic respiration (source)
89 resulting from warming versus enhanced photosynthesis (sink) resulting from the direct effects
90 of elevated CO_2 and warming on production and from the acceleration of nutrient cycles by
91 warming (McKane et al., 1997, Rastetter et al., 1997, McGuire et al., 2012, Pearce et al., 2015,
92 Jiang et al., 2017). This trade-off between source versus sink activity is likely to be confounded
93 by arctic herbivores.

94 From the perspective of ecosystem biogeochemistry, aggregating herbivore effects in
95 with other processes can be justified because grazers perform several nutrient-cycling processes
96 that parallel other plant and microbial processes within ecosystems. Here we examine
97 aggregation effects for four such processes in relation to the response of ecosystems to elevated
98 CO_2 and warming: (1) Grazing mediates the transfer of plant C to detritus and soil organic matter
99 (soil), and thereby acts in parallel with tissue senescence and litter fall. (2) Similarly, grazing
100 transfers plant N to soil organic matter in parallel with tissue senescence and litter fall, but does
101 so before the plants can resorb N. (3) Consumption of plant material and subsequent
102 heterotrophic respiration by grazers parallels litter fall and the subsequent heterotrophic
103 respiration resulting from processing of soil organic matter by microbes and other detritivores.
104 (4) Finally, metabolic processing of plant matter consumed by grazers produces dissolved labile
105 N in urine in parallel with litter fall and microbially mediated mineralization.

106 Even though these processes act in parallel, the grazer-mediated and non-grazer-mediated
107 processes might respond differently to climate change, or even in opposite directions.
108 Furthermore, the cyclic dynamics of small-mammal grazers in the Arctic might complicate the

relative contributions of these parallel processes to ecosystem responses to elevated CO_2 and climate change. Based on the modeling analysis we present below:

(1) We hypothesize that aggregating the effects of small-mammal grazers with other C and N cycling processes results in an underestimation of tundra responses to elevated CO_2 and warming. For our model, after 100 years the underestimation of C sequestration in tundra ecosystems in response to elevated CO_2 and warming is 50 to 80% relative to estimations in which the grazer effects are explicitly represented.

(2) We hypothesize that although three-to-four-year cycles in the density of small-mammal grazers have measurable short-term effects of tundra biogeochemistry (e.g., Olofsson et al. 2012), densities averaged over the grazer cycles can be used to assess long-term responses of tundra to elevated CO_2 and warming.

We use a simple model of coupled C and N cycles in ecosystems applied to the effects of small-mammal grazers on the responses of moist acidic tundra to elevated CO_2 and warming. Most of the data we use is for lemmings and voles, but the model applies to generic small-mammal grazers in the Arctic, which we refer to as "voles" for simplicity. We apply the model both with vole densities explicitly represented and with vole densities unspecified, but their effects implicitly subsumed into other biogeochemical processes. In all applications of the model, we assume voles are present on the landscape. The model applications differ only in the way that vole and other biogeochemical processes are separated from one another.

METHODS

Model: We use a model developed by Rastetter et al., (2020) to examine recovery of ecosystems from disturbances that remove vegetation (Box 1, Rastetter et al. 2021a). We have modified that model to account for temperature sensitivity of six metabolic processes (photosynthesis, autotrophic and heterotrophic respiration, plant and microbial N uptake, and N mineralization). We have also modified it to account for the effects of voles on the transfer of C and N from vegetation to soil organic matter and the transfer of N in urine from vegetation to inorganic N (although not all N in urine is inorganic, it is labile, and we treat it as inorganic). The basic model is fully described in Rastetter et al., (2020); here we describe only the changes to that model for the current analyses.

Temperature response of metabolic processes: Because we use an annual time step in the model (i.e., no seasonality) and restrict warming to 5 ^{o}C above current temperatures, we use a simple Q_{10} function to simulate temperature responses rather than more complex formulations (e.g., Heskel et al., 2016 or Carey et al., 2016). We have therefore modified the photosynthesis, autotrophic respiration, heterotrophic respiration, plant N uptake, microbial N uptake, and N mineralization in the Rastetter et al., (2020) model to increase exponentially with warming (Box 1: Eqs. 9, 10, 13, 14, 19, and 20).

Vole grazing: We drive the model by specifying vole density in each year (V). Consistent with values and cycle frequency reported in the literature (Batzli et al., 1980, Krebs et al., 1995, Korpimaki et al., 2004, Pitelka and Batzli 2007, Krebs 2013, Ehrich et al. 2020), we use a randomly generated time series of vole abundance with peaks every three or four years, with abundances at the peak ranging from 90 to 110 voles ha^{-1}, minimum abundances ranging from 8 to 12 voles ha^{-1}, and a mean vole abundance over the full time series of 40 voles ha^{-1} (Fig. 1). We chose to take this prescribed approach to vole density because the drivers of vole cycles

154 are not fully understood (Korpimaki et al., 2004, Prevedello et al., 2013, Oli 2019) and likely
155 include a top-down component (Pitelka et al., 1955, Hairston et al., 1960, Krebs 2013), which is
156 well beyond the domain of our model. For convenience, we specify vole density in voles ha^{-1}
157 and correct to m^{-2} units by dividing by 10,000 m^2 ha^{-1} (Eqs. 15, 17, & 18).
158 The removal of C from vegetation for nest building and ingestion are lumped into a
159 single process for our model (Eq. 15). We assume this C removal is proportional to the specified
160 vole density but decrease the per capita rate of ingestion with warming to account for decreased
161 energy requirements to maintain body temperature (Eq.15; Batzli et al., 1980). Vole respiration
162 is proportional to the ingestion component of C removal from vegetation by voles and therefore
163 also declines with warming (Eq. 17). We do not account for other temperature responses like
164 those associated with cold or heat stress. We assume a constant C:N ratio of material removed
165 from vegetation by grazers (Eq. 16) but, because of the respiration loss of C and the N
166 transferred to inorganic N in urine, the C:N of material removed from vegetation and the C:N of
167 material added to the soil organic matter differ. Finally, we assume urine losses of N are
168 proportional to vole density (Eq. 18).
169
170 **Model calibration:** We calibrate the model to be consistent with the C and N stocks and
171 process rates compiled by Pearce et al., (2015) for the Multiple Element Limitation (MEL)
172 model (Table 1). Because voles are part of the ecosystem, the effects of voles on tundra C and N
173 stocks and fluxes are implicitly included in the data compiled by Pearce et al.,
174 (2015). Therefore, by using these data to calibrate (fit) the model without explicit vole
175 representation, we are implicitly aggregating those vole effects in with the parallel ecosystem
176 processes described above. In the calibrations in which voles are explicitly represented, we

assume a constant vole density and that the ecosystem is in steady state. We then specify the vole effects directly and subtract these effects from the parallel ecosystem processes before calibration (Table 2). The combined rates of vole-mediated processes plus the parallel ecosystem processes are therefore identical in all calibrations (rows labeled "Total" in Table 2), thus providing the basis of comparison for assessing the consequences of explicit versus aggregated representation of vole grazing.

In the calibrations, first we set allometric, C:N, Q_{10}, half-saturation, and vole-related parameters (derivation of these parameter values is presented in Appendix S1). We then set the rate parameters for each process so that flux rates are consistent with rates reported in Pearce et al., (2015). Because annual rates of plant and microbial processes are dominated by growing-season rates, we use average summer temperature (10 ^{o}C) to calibrate the model; in any case, because of the Q_{10} formulation, once calibrated to a specified temperature, model responses are sensitive to changes in temperature, not to the temperature value itself. For vole processes, we correct this summer temperature to average annual temperature with an off-set (Eq. 15).

We made three calibrations (Tables 3 & 4). In calibration I, vole densities are not explicitly specified, and we assume that vole-mediated processes can be implicitly represented by aggregating them with the parallel biogeochemical processes described in the introduction above (Table 2). In this calibration, we therefore set the number of voles (V) in the model to zero but incorporate the effects of voles in with the parallel processes through the calibration. In calibration II, we set the number of voles to 40 voles ha^{-1} so that vole-mediated processes are explicitly represented, and the number of voles is the mean abundance of voles we use in our simulated vole cycle (described above). In calibration III, we set the number of voles to 100 voles ha^{-1}, which is the mean peak-vole abundance in our simulated vole cycle. In calibration

III, the parallel ecosystem process rates are decreased proportionally more than in calibration II to account for the higher vole density (Table 2).

All but four of the parameters have the same values in all three calibrations. To maintain the same steady state in all three calibrations, we adjust the values of these four parameters to compensate for how voles are represented in the model (m_{CB}, m_{NB}, r_D, and m_{Nm}; rows labeled "PAR" in Table 2). These parameters are adjusted so that the rates of C and N litter losses, heterotrophic soil respiration, and gross N mineralization all decrease to compensate for the parallel vole-mediated C and N fluxes in calibrations II and III where voles are explicitly represented. Because we calibrate to the same data set (Pearce et al., 2015), the overall C and N stocks and cycling rates are identical for these three calibrations (rows labeled "Total" in Table 2).

Simulations: We run a total of thirteen simulations in two sets (Tables 3 & 4, Rastetter et al. 2021b&c).

In the first set of simulations, we assume that the average vole density is 40 voles ha^{-1} and use calibration II with vole effects explicitly represented (Table 3). We then run four 200-year simulations with no change in either CO_2 or temperature. We drive the model with: (1) voles held constant at 40 voles ha^{-1}; (2) voles cycling on the three-to-four-year cycle between 8 and 110 voles ha^{-1} for 200 years; (3) voles cycling for ten years, followed by maintenance of a constant vole density of 100 voles ha^{-1} (equivalent to adding voles to the ecosystem); and (4) voles cycling for ten years, followed by maintenance of a constant vole density of 0 voles ha^{-1} (equivalent to removing voles from the ecosystem).

222 This first set of simulations serves two purposes. First, it illustrates the effects of long-
223 term changes in vole density and thereby draws the distinction between adding or removing
224 voles from calibrating the model assuming high or low vole density. Second, it allows us to
225 assess the potential long-term effects of voles if their numbers were maintained at high or low
226 levels. We can thereby address the question: "Do the simulated changes in the ecosystem
227 approach their potential changes during peaks and troughs in the vole cycle?"
228 The second set of simulations is to address our central question about aggregated versus
229 explicit representations of grazer effects on ecosystem responses to climate change (Table 4).
230 We run nine 100-year simulations in a two-factor design. The first factor relates to how vole
231 effects are represented in the three calibrations (Table 3) and vole abundance: (1) calibration I
232 (aggregated) and vole abundance subsumed in the calibration of the parallel processes and
233 therefore assumed constant but unspecified (although V is set to 0 in the model, vole effects are
234 aggregated in with the parallel ecosystem processes); (2) calibration II (40 voles ha^{-1}) and vole
235 abundance cycling on the three-to-four-year cycle between 8 and 110 voles ha^{-1}; and (3)
236 calibration III (100 voles ha^{-1}) and vole abundance held constant at 100 voles ha^{-1}. The second
237 factor relates to climate change: (1) a linear increase in atmospheric CO_2 from 400 to 800 μmol
238 mol^{-1} over 100 years; (2) a linear increase in temperature from 10 to 15 ºC over 100 years; and
239 (3) a linear increase in both atmospheric CO_2 from 400 to 800 μmol mol^{-1} and temperature from
240 10 to 15 ºC over 100 years.
241
242 **RESULTS**
243 **Set 1: Effects of vole cycling and adding or removing voles.**

244 *Simulation 1: Effects of holding voles constant at the calibration abundance.* Because
245 the model was calibrated to a steady state with 40 voles ha^{-1}, all ecosystem C and N stocks and
246 fluxes remained constant when vole abundance was held at 40 voles ha^{-1} in the 200 year
247 simulations (dotted horizontal lines in Fig. 2). This simulation only serves to illustrate the
248 stability of the model and to serve as a control to which the other simulations can be compared.
249 *Simulation 2: Effects of vole cycling on plant and soil C and N*. In the 200-year
250 simulations with vole abundance cycling, the plant and soil C and N stocks cycle at the same
251 three-to-four-year frequency as the voles (Fig. 2). In addition, there are some longer-term
252 dynamics in these stocks associated with the auto-correlated nature of plant production and the
253 legacy of the random variations in the vole cycle. Despite these dynamics, vole cycling does not
254 cause the plant and soil C and N stocks to diverge far from the values to which they are
255 calibrated (dotted and solid lines in Fig. 2).
256 The plant biomass cycles out of phase with the vole cycle. The lowest plant C and N
257 values occur in years of peak vole numbers and the highest plant C and N values occur three or
258 four years after peak vole numbers or the year prior to the subsequent vole peak (Fig. 3). This
259 phase shift in the plant relative to vole cycles as well as the magnitude of the plant C cycle (20 to
260 30 g C m^{-2} peak to trough) are roughly consistent with the phase and magnitude of the cycles
261 reported by Olofsson et al., (2012). In addition, the dependence of plant production on plant
262 biomass results in a strong autocorrelation in the plant C and N time series, which in turn results
263 in longer-term dynamics less clearly tied to the vole cycle (Fig. 2). This autocorrelation is
264 reflected in the strong positive correlation between the plant C and N and their respective values
265 at the time of the previous peak in vole numbers (open dots remain high and closed dots remain
266 low in Fig. 3).

The dynamics of soil C and N stocks are closely tied to the plant dynamics. Because N inputs to the ecosystem are less than 3% of the annual plant requirement (Table 1), plant recovery from vole outbreaks relies almost exclusively on N from soil organic matter. As a consequence, the three-to-four-year soil N cycles are directly out of phase with plant N cycles and the longer-term dynamics are also opposite those in plant N (Fig. 2). Soil C also cycles out of phase with plant C, but the relation is not as strong as it is for N. However, because soil C is ultimately derived from plant C, the longer-term dynamics in plant C are paralleled in the soil C following about a 9-year lag (Fig. 2).

Simulations 3 & 4: Effects of removing or adding voles. When voles are removed from the ecosystem, plant C and N increase by about 13%, or increase by 116 g C m^{-2} and 2.7 g N m^{-2}. Because of the reliance of plants on soil N, soil N deceases by almost the same absolute amount as the plants gain, 2.5 g N m^{-2}. However, the amount of N in the soil is so large that this loss amounts to only about a 0.3% loss. The increase in plant biomass results in higher litter inputs to the soil. Consequently, soil C increases by about 4% or 727 g C m^{-2}. The gain of soil C and loss of soil N widens the soil C:N ratio by about 4%, which in turn increases microbial N immobilization into soil organic matter (effect of Φ in Eq. 14).

When voles are increased and then held constant at 100 voles ha^{-1}, plant C and N decrease by about 20%, or 175 g C m^{-2} and 4 g N m^{-2}. Again, because of the tight cycling of N in the ecosystem, soil N increases by almost the same absolute amount as the plants lose, 3.7 g N m^{-2} (0.4%). The loss of plant biomass translates into lower litter inputs to soil and a large absolute decrease in soil C, 1170 g C m^{-2} (6%). Because of the increase in soil N and decrease in soil C, the soil C:N narrows by about 6%, which in turn decreases microbial N immobilization into soil organic matter (effect of Φ in Eq. 14).

290 In the simulations where vole density is increased or decreased and then held constant, it
291 takes 10 to 20 year for the vole effects to reach their largest deviation from the steady state and
292 another 60 to 90 years for those effects to stabilize. Because of this long response time, the
293 potential effects of voles on tundra biogeochemistry cannot be approached if vole abundance
294 cycles on a three-to-four-year cycle. Indeed, when voles are cycling, the magnitude of these
295 effects relative to the peak effects of the long-term increase or decrease in vole abundance is only
296 about 12% for plant C, 2% for soil C, and 20% for both plant and soil N.

297 **Set 2: Effects of aggregated versus explicit representations of vole effects.**

298 *Simulations 5, 8, & 11: Responses to increasing CO_2.* Predicted responses to increased
299 CO_2 do not differ substantially between the aggregated model in which vole effects are implicitly
300 aggregated in with other biogeochemical processes through model calibration (calibration I) and
301 the distributed model in which vole effects are explicitly represented (calibrations II & III: Figs.
302 4, 5, & 6). The only process affected by elevated CO_2 is photosynthesis. However, because the
303 plants are strongly N limited, elevated CO_2 increases net primary production (NPP) by only 10-
304 11% in both aggregated and distributed simulations (Fig. 6). This increase in production
305 translates into about an 11-12% increase in biomass, again in both aggregated and distributed
306 simulations (Fig. 4). The increase in production results in only about a 4% increase in soil C in
307 all the simulations. This increase in soil C is a small relative change but, because soil has such a
308 large fraction of the organic matter, it is a large absolute change amounting to about 90% of the
309 total change in ecosystem C.

310 The amount of N entering the ecosystem is too small to support even the small gain in
311 plant C in response to elevated CO_2. The gain is instead supported by a net transfer of 0.9 - 1.3 g
312 N m^{-2} from soil to plants over the 100-year simulations. The amount of N transferred from soil

313 to plants is about the same in all three simulations (Fig. 5). Elevated CO_2 increases the C:N ratio
314 of the plants, which in turn increases N uptake (effect of Ψ in Eq. 10). However, the increase in
315 soil C:N resulting from increased litter inputs also increases microbial N uptake (effect of Φ in
316 Eq. 14). This competition between plants and microbes for N limits the ecosystem response to
317 elevated CO_2. Again, the effects of aggregated versus explicit representation of voles on this
318 response to elevated CO_2 are negligible (Figs. 4, 5, & 6).
319 *Simulations 6, 9, & 12: Responses to warming.* In contrast, the effects of aggregated
320 versus explicit representation of voles on the response to warming are large (Figs. 4, 5, & 6).
321 Warming not only stimulates photosynthesis, it also stimulates autotrophic and heterotrophic
322 respiration, and, more importantly, it stimulates the N cycle in three places: (1) N mineralization,
323 (2) microbial N uptake, and (3) plant N uptake. A major effect of this stimulation of the N cycle
324 is an increase in net N mineralization, a resulting relaxation of N limitation on plant growth, and
325 a large increase in plant biomass. The increase in plant production increases litter inputs to soils,
326 which in turn mitigates soil C losses. In addition, the increased production allows the ecosystem
327 to accumulate a small amount of N (<0.3 g N m^{-2}; Fig. 6). The effects of this chain of events are
328 much stronger in the simulations where voles are explicitly represented than in the simulations
329 with the aggregated model and the effects are stronger when the model is calibrated assuming
330 higher vole densities (response stronger for calibration III [100 vole ha^{-1}] than for calibration II
331 [40 voles ha^{-1}]). Thus, explicit representation of vole effects results in an amplification of the
332 predicted transfer of N from soil to plants, larger predicted gains in plant C or higher predicted
333 retention of soil C, and higher predicted rates of gross primary production (GPP), net primary
334 production (NPP), and net ecosystem production (NEP). If the simulations are run with vole
335 density held constant at 40 voles ha^{-1}, the C and N stocks and fluxes follow the same general

patterns as in the simulations with the three-to-four-year vole cycle (data not shown). The size of the differences between the simulations with constant 40 voles ha^{-1} and cycling vole density are about the same as those of the cycle simulation from the steady state with no climate change (Fig. 2). In addition, the temperature effects on vole consumption and respiration (Box 1, Eqs. 15 & 17) have only a small effect on this general pattern (simulations rerun with $\varepsilon_V = 0$ resulted in < 2% difference in C and N stocks; data not shown).

Simulations 7, 10, & 13: Responses to increasing CO_2 and warming. The effects of elevated CO_2 and warming are slightly amplified when the two are combined (the two interact synergistically). Under both elevated CO_2 and warming, GPP is 12% and NPP is 8% higher than the sum of the changes in GPP and NPP under elevated CO_2 alone and warming alone (Fig. 6). The net transfer of N from soil to plants is about 3% stronger and the increase in plant C is about 7.5% stronger (Fig. 4 & 5). Overall, because the response to CO_2 alone is so much smaller that the response to warming alone, the response to the two combined is dominated by the warming response. The consequences of aggregated versus explicit representations of vole effects are therefore the same as in the warming simulations.

In our analysis we assume vole density is top-down controlled and therefore does not increase with plant production. However, if the average vole density during the cycle increases in proportion to NPP (~80% over 100 years), some of the increased production with elevated CO_2 and warming is consumed and the increase in plant biomass is about 7.6% lower than when the average vole density remains constant (data not shown). The increase in vole density causes soil C to decrease by 0.9% rather than increase by 0.4%.

DISCUSSION

359 Our analysis indicates that failure to explicitly represent small-mammal grazers (voles) in
360 biogeochemical models can result in an underestimation of the response of arctic ecosystems to
361 climate warming but has only a small effect on the response to elevated CO_2 (Fig. 4, 5, & 6).
362 Underestimation of the warming response increases with the assumed density of voles used to
363 calibrate the model. Although cycling of vole density has short-term effects on ecosystem stocks
364 and fluxes, it neither amplifies nor dampens the underestimation in the long-term response to
365 warming. Why is the explicit representation so important?
366 Before addressing this question, we again emphasize the distinction between explicit
367 representation of voles and adding voles to the ecosystem. Adding voles to the ecosystem
368 accelerates nutrient cycling by increasing the transfer of nutrients from plants to soil. Such an
369 acceleration of nutrient cycling might be expected to increase the responsiveness to elevated CO_2
370 and warming. However, in our analysis of the response to elevated CO_2 and warming we do not
371 add voles; we simply change how the voles are represented in the model. Vole effects are either
372 implicitly aggregated in with other processes or they are explicitly represented. In all three of
373 our calibrations, the total amounts of C and N removed from vegetation, the total heterotrophic
374 respiration, and the total mineralization of N are identical (Table 2). Thus, the *magnitudes* of
375 vole-mediated processes plus the parallel ecosystem processes are represented identically in all
376 three calibrations. Furthermore, in the analysis where we did add voles, any acceleration of
377 nutrient cycles by vole activity is transient; our analysis indicates that the net effect of adding
378 voles is to transfer N from plants, with relatively high N turnover, to soil, with slower N turnover
379 (Fig. 2); although it would be impossible to detect the 0.6% change in soil N predicted by our
380 model. Thus, the long-term effect of adding voles is to slow the nutrient cycle. Furthermore,
381 adding and maintaining 100 voles ha^{-1} resulted in a loss of over a kilogram of C from the

ecosystem (Fig. 2). Thus, the effect of adding grazers is to *decrease* ecosystem C whereas explicitly representing voles in the model is to *increase* the estimate of C gain with climate change (Fig. 4).

Why are the differences in responses to elevated CO_2 so small between aggregated versus explicit representation of vole effects? Elevated CO_2 stimulates only one ecosystem process, photosynthesis (Fig. 7). The associated increase in C gain increases biomass and leaf area, which further stimulates photosynthesis (Fig. 7: $\uparrow C_a \rightarrow \uparrow P_s \rightarrow \uparrow B_C \rightarrow \uparrow S \rightarrow \uparrow P_s$). However, there is a much stronger negative feedback associated with the change in stoichiometry; increased photosynthesis increases biomass C and consequently increases vegetation C:N, which feeds back to decrease photosynthesis ($\uparrow C_a \rightarrow \uparrow P_s \rightarrow \uparrow B_C \rightarrow \uparrow \Psi \rightarrow \downarrow P_s$). Tissue and Oechel (1987) used this stoichiometric feedback to argue why tussock tundra exposed to elevated CO_2 alone had only a transient increase in production. Without an increase in the N supply to vegetation, the CO_2-stimulation of photosynthesis cannot be maintained. However, the increase in vegetation C:N increases the litter-fall C:N and consequently the soil C:N, which in turn decreases net N mineralization and the supply of N to plants ($\uparrow C_a \rightarrow \uparrow P_s \rightarrow \uparrow B_C \rightarrow \uparrow \Psi \rightarrow \downarrow L_{itN} \rightarrow \downarrow D_N \rightarrow \uparrow \Phi \rightarrow \downarrow (N_{min}\text{-}U_{Nm})$). Because none of the steps in this chain were modified to incorporate voles explicitly in the model calibration, this N feedback is about the same for both explicit and aggregated representation of voles in the model and therefore does not have a large effect on the relative responses with and without explicit representation of vole effects.

Why are the predicted responses to warming stronger when vole effects are explicitly represented in the model than when they are aggregated with other processes? In

405 the model, warming stimulates six processes: photosynthesis, autotrophic and heterotrophic
406 respiration, N mineralization, microbial N uptake, and plant N uptake (Fig. 7). Although
407 warming decreased the energy cost of thermoregulation and therefore decreases vole
408 consumption of plants (Eq. 15) and vole respiration (Eq.17), we found that this effect is too small
409 to explain the differences between simulations with versus without voles explicitly represented
410 (accounting for < 2% of the response in C and N stocks).
411 Among these many effects of warming in the model, the main effect that results in the
412 accumulation of plant C in simulations with both explicit and aggregated representations of vole
413 effects is the release from N limitation through the stimulation of net N mineralization (Fig. 7:
414 $\uparrow T \rightarrow \uparrow(N_{min}\text{-}U_{Nm}) \rightarrow \uparrow N \rightarrow \uparrow U_N \rightarrow \uparrow B_N \rightarrow \downarrow \Psi \rightarrow \uparrow P_s$). Thus, one effect of this mobilization of
415 soil N is for both C and N uptake by plants to increase, causing plant biomass to accumulate.
416 Because N mineralization (N_{min}) was decreased in calibrations II and III to accommodate the
417 explicit representation of voles (Table 2), this warming-induced growth in plant biomass is about
418 0.8% (40-vole calibration II) to 2% (100-vole calibration III) weaker in the simulations with the
419 explicit representation of vole effects. These simulations nevertheless accumulate more, not less,
420 biomass.
421 The main reason that plant C and N accumulation differed between simulations with
422 aggregated versus explicit representations of voles is the change made to litter fall rates to
423 accommodate the voles in calibrations II and III (Table 2). Litter fall is not directly stimulated
424 by warming (Eqs. 11 & 12), but it does increase as plant biomass increases. This increase in
425 litter fall in turn limits the amounts of C and N that can accumulate in plants. However, the
426 fraction of plant C and N lost in litter fall was decreased in calibrations II and III in which voles
427 are explicitly represented to accommodate the C and N consumed by voles (Table 2: m_{CB} & m_{NB}

were decreased). Consumption by voles does not increase with plant biomass (Eq. 15), and vole density does not increase with plant biomass because we assume top-down control on voles and therefore use a prescribed vole density. As a consequence, the increase in litter fall as biomass accumulates is smaller with voles explicitly represented than in the aggregate representation. The accumulation of C and N in vegetation is therefore larger with the explicit inclusion of vole effects than in the simulation where vole effects are aggregated with other processes. When we do allow vole density to increase in proportion of the increase in NPP (~80% over 100 years), the increase in plant biomass is less than 8% lower because of consumption and the small increase in soil C (<0.5%) becomes a small decrease (<1%).

In addition, because the C:N ratio of forage (19.15 g C g^{-1} N) is lower than the C:N ratio of litter (40 g C g^{-1} N), the fraction of vegetation N lost in litter fall was decreased more than the fraction of vegetation C lost in litter fall in calibrations II and III with explicit vole representations (Table 2; e.g., 13.7% decrease in litter N versus 6.6% decrease in litter C with 40 vole ha^{-1}). As a consequence, as vegetation biomass accumulates, the litter-fall C:N ratio increases more with the explicit representation of voles than with aggregated representation of vole effects. Soil organic C therefore increases more with the explicit vole representation than without it (Fig. 4), and soil organic N decreases more with the explicit vole representation than without it (Fig. 5).

Why is there a synergistic response to elevated CO_2 and warming in combination?

If the response to CO_2 were stronger so that there was a substantial increase in plant biomass and plant C:N ratio, then the feedback associated with litter fall would have come into play and differences between explicit and aggregated representations of vole activity would have made

more of a difference by the same mechanism described above for the response to warming. When elevated CO_2 is combined with warming, the warming mobilizes soil N, easing N limitation of plant production, and the inhibiting feedback on production associated with higher plant C:N is weakened. This weakening of the C:N feedback allows the direct effects of elevated CO_2 to be more strongly manifested, and hence a stronger response to both elevated CO_2 and warming than the sum of the responses to each factor individually. Tissue and Oechel (1987) found the same synergistic effect resulting in a sustained increase in production with elevated CO_2 and warming but only a transient increase with CO_2 alone.

CONCLUSIONS

Grazing animals can have large effects on ecosystems (Grellman et al., 2002, McLaren and Jefferies 2004, Sjögersten et al., 2008, Post and Pedersen 2008, Rinnan et al., 2009, Cahoon et al., 2011, Kaarlejärvi et et al., 2015, Leffler et al., 2019, Min et al., 2021). Our simulations suggest that long-term exclusion of voles or maintenance of vole populations at high densities can result in large gains or losses of both plants and soil C (Fig. 2). However, the response time of plants and soil to these persistent changes in grazing takes several decades in our model. As a consequence, the full effect of changes in vole densities are never realized when voles cycle on a three-to-four-year time scale. Indeed, cycling at such a high frequency can be incorporated in our model using the long-term mean density without any substantial change in the predicted long-term dynamics of the ecosystem. Our simulations excluding and including voles are not purely academic. Recent studies suggest that arctic rodent population cycles could dampen in amplitude or be punctuated with periods of non-cyclic dynamics in response to altered climate conditions, in particular changes in snow conditions (Gilg 2006, Ims et al., 2008, Kausrud 2008,

474 Brommer et al., 2010, Domine 2018). Our results suggest that the important dynamics for
475 predicting long-term changes in tundra biogeochemistry in response to climate change are the
476 mean grazer dynamics on decadal scales, not the higher frequency three-to-four-year cycles.
477 The effects of voles on C and N cycling can have major effects on the biogeochemical
478 responses of tundra to elevated CO_2 and warming. These effects need to be explicitly
479 represented in models rather than aggregated with other ecosystem processes. Even if these
480 other processes act in parallel with vole processes, their response to changes in the environment
481 can be very different. Our analysis indicates that failure to explicitly account for voles results in
482 large underestimation of the responses of tundra to climate warming and to elevated CO_2 and
483 warming. Our analysis is analogous to that of Thornton et al., (2007) who found that predicted
484 responses of the terrestrial biosphere to elevated CO_2 and climate change was likely
485 overestimated unless N limitation was explicitly represented in models. We recommend that
486 grazing effects be explicitly incorporated when applying models of tundra response to global
487 change.
488 Our analysis is based on a simple, annual-time-step model of ecosystem C and N
489 interactions calibrated to arctic tundra. The simplicity of the model facilitates causal tracing
490 (Fig. 7) and heuristic analysis of the results, but at the expense of quantitative detail in the
491 dynamics (Rastetter 2017). The results should therefore be confirmed for more complex models
492 with, for example, more detailed representations of vegetation and soil characteristics, finer-scale
493 seasonal dynamics, and the effects animals can have on plant-community composition and soil
494 structure. Although our model was calibrated for arctic tundra, the qualitative conclusions
495 probably apply more broadly. In our analysis, a key process is vole respiration, which decreases
496 with warming, unlike the increase with warming for plant and microbial respiration. This

property is clearly relevant to mammal grazers in cold climates, but not for mammal grazers in warm climates or for insects in any climate. Nevertheless, for these other ecosystems there might be analogous model biases associated with aggregating biogeochemical processes mediated by these grazers with other ecosystem processes. Similarly, the consequences of resource limitation need to be examined for grazers in ecosystems that are bottom-up regulated. All these possibilities need to be analyzed, first with heuristic models like the one we use and then incorporated into more detailed biogeochemical models. To perform these analyses, more data like those in Batzli et al. (1980) and Olofsson et al. (2012) are needed that can be directly applied in these biogeochemical models. Collection of these data will require a biogeochemical, as well as a community, perspective on plant-grazer interactions.

ACKNOWLEDGEMENTS

This work was supported in part by the National Science Foundation under NSF grants 1651722, 1637459, 1603560, 1556772, 1841608 to E.B.R.; 1603777 to N.T.B. and K.L.G.; 1603654 to R.J.R.; 1603760 to L.G.; 1603677 to J.R.M. Any opinions, findings and conclusions or recommendations expressed in this material are those of the authors and do not necessarily reflect those of the National Science Foundation. We also want to thank Bonnie Kwiatkowski for assistance with code development and archiving.

LITERATURE CITED

Batzli, G. O., R. G. White, S. F. MacLean Jr, F. A. Pitelka, and B. D. Collier. 1980. The herbivore-based trophic system. pp 335-410 in Brown, J., Miller, P.C., Tieszen, L.L., and Brunnell, F.L. eds.. An Arctic Ecosystem: the Coastal Tundra at Barrow, Alaska. Dowden, Hutchinson, and Ross Inc, Stroudsburg, PA, USA

Bennett, V. J. 2003. Computer modelling the Serengeti-mara ecosystem. Doctor of Philosophy dissertation, School of Biology, The University of Leeds.

Brommer, J. E., H. Pietianen, K. Ahola, P. Karell, T. Karstinen, and H. Kolunen. 2010. The return of the vole cycle in southern Finland refutes generality of the loss of cycles through 'climatic forcing'. Global Chance Biology 16:577-586

Cahoon, S. M. P., P. F. Sullivan, E. Post, and J. M. Welker. 2011. Large herbivores limit CO2 uptake and suppress carbon cycle responses to warming in West Greenland. Global Change Biology 18:469–479.

Carey, J. C., J. Tang, P. H. Templar, K. D. Kroger, T. W. Crowther, A. J. Burton, J. S. Dukes, B. Emmett, S. D. Frey, M. A. Heskel, L. Jiang, M. B. Machmuller, J. Mohan, A. M. Panetta, P. B. Reich, S. Reinsch, X. Wang, S. D. Allison, C. Bamminger, S. Bridgham, S. L. Collins, G. de Dato, W. C. Eddy, B. J. Enquist, M. Estiarte, J. Harte, A. Henderson, B. R. Johnson, K. S. Larsen, Y. Luo, S. Marhan, J. M. Melillo, J. Peñuelas, L. Pfeifer-Meister, C. Poll, E. Rastetter, A. B. Reinmann, L. L. Reynolds, I. K. Schmidt, G. R. Shaver, A. L. Strong, V. Suseela, and A. Tietema. 2016. Temperature response of soil respiration largely unaltered with experimental warming. Proc Nat Accad Sci 113:13797-13802.

539 Domine, F., Gauthier G., Vionnet V., Fauteux D., Dumont M., and Barrere M. 2018. Snow
540 physical properties may be a significant determinant of lemming population dynamics in
541 the high Arctic, Arctic Science, 4: 813–826 https://doi.org/10.1139/as-2018-0008
542 Ehrich, D., N.M. Schmidt, G. Gauthier, R. Alisauskas, A. Angerbjörn, K. Clark, F. Ecke, N.E.
543 Eide, E. Framstad, J. Frandsen, A. Franke, O. Gilg, M.A. Giroux, H. Henttonen, B.
544 Hörnfeldt, R.A. Ims, G.D. Kataev, S.P. Kharitonov, S.T. Killengreen, C.J. Krebs, R.B.
545 Lanctot, N. Lecomte, I.E. Menyushina, D.W. Morris, G. Morrisson, L. Oksanen, T.
546 Oksanen, J. Olofsson, I.G. Pokrovsky, I.Y. Popov, D. Reid, J.D. Roth, S.T. Saalfeld, G.
547 Samelius, B. Sittler, S.M. Sleptsov, P.A. Smith, A.A. Sokolov, N.A. Sokolova, M.Y.
548 Soloviev, D.V. Solovyeva. 2020. Documenting lemming population change in the Arctic:
549 Can we detect trends? Ambio 49:786-800. doi: 10.1007/s13280-019-01198-7.
550 Gilg, O., B. Sittler, and I. Hanski. 2009. Climate change and cyclic predator–prey population
551 dynamics in the high Arctic. Glob. Change Biol. 15, 2634–265210.1111/j.1365-
552 2486.2009.01927.x doi:10.1111/j.1365-2486.2009.01927.x.
553 Gough, L., J. C. Moore, G. R. Shaver, R. T. Simpson, and D. R. Johnson. 2012. Above- and
554 belowground responses of arctic tundra to altered soil nutrients and mammalian
555 herbivory. Ecology 93:1683-1694.
556 Grellman, D. 2002. Plant responses to fertilization and exclusion of grazers on an arctic tundra
557 heath. Oikos, 98:190–204.
558 Hairston, N. G., F. E. Smith, and L. B. Slobodkin. 1960. Community structure, population
559 control, and competition. The American Naturalist 94:421–425.
560 Heskel, M. A., O. S. O'Sullivan, P. B. Reich, M. G. Tjoelker, L. K. Weerasinghe, A. Penillard, J.
561 J. G. Egerton, D. Creek, K. J. Bloomfield, J. Xiang, F. Sinca, Z. R. Stangl, A. Martinez-

562 de la Torre, K. L. Greffin, C. Huntingford, V. Hurry, P. Meir, M. H. Turnbull, and O. K.
563 Atkin. 2016. Convergence in the temperature response of leaf respiration across biomes
564 and plant functional types. Proc Nat Accad Sci 113: 3832-3837.
565 Ims, R. A., J. A. Henden, and S. T. Killengreen. 2008. Collapsing population cycles. Trends
566 Ecol. Evol. 23, 79–8610.1016/j.tree.2007.10.010 doi:10.1016/j.tree.2007.10.010.
567 Jai, S., X. Wang, Z. Yuan, F. Lin, Z. Hao, and M.S. Luskin. 2018. Global signal of top-down
568 control of terrestrial plant communities by herbivores. Proceedings of the National
569 Academy of Sciences 115, 6237-6242. DOI: 10.1073/pnas.1707984115.
570 Jiang, Y., E. B. Rastetter, G. R. Shaver, A. V. Rocha, Q. Zhuang, and B. L. Kwiatkowsk. 2017.
571 Modeling long-term changes in tundra carbon balance following wildfire, climate change
572 and potential nutrient addition. Ecological Applications 27:105-117
573 Kaarlejärvi, E., K. S. Hoset, and J. Olofsson. 2015. Mammalian herbivores confer resilience of
574 arctic shrub-dominated ecosystems to changing climate. Global Change Biology 21,
575 3379-3388.
576 Kausrud, K. L., A. Mysterud, H. Steen, J. O. Vik, E. Ostbye, B. Cazelles, E. Framstad, A. M.
577 Eikeset, I. Mysterud, T. Solhoy, and N. C. Stenseth. 2008. Linking climate change to
578 lemming cycles. Nature 456, 93–9710.1038/nature07442 doi:10.1038/nature07442.
579 Korpimaki, E., P. R. Brown, J. Jacobs, and R. P. Pech. 2004. The puzzles of population cycles
580 and outbreaks of small mammals solved? Bioscience 5412.:1071-1079
581 Krebs, C. J. 2013. Population fluctuations in rodents. University of Chicago Press, Chicago, IL
582 USA

583 Krebs, C. J., R. Boonstra, and A. J. Kenney. 1995. Population dynamics of the collared lemming
584 and the tundra vole at Pearce Point, Northwest Territories, Canada. Oecologia 103:481-
585 489.
586 Leffler, A. J., K. H. Beard, K. C. Kelsey, R. T. Choi, J. A. Schmutz, and J. M. Welker. 2019.
587 Delayed herbivory by migratory geese increases summer-long CO2 uptake in coastal
588 western Alaska. Global Change Biology, 25, 277–289.
589 Legagneux, P., G. Gauthier, D. Berteaux, J. Bêty, M. C. Cadieux, F. Bilodeau, E. Bolduc, L.
590 McKinnon, A. Tarroux, J. F. Therrien, L. Morissette, and C. J. Krebs. 2012.
591 Disentangling trophic relationships in a high arctic tundra ecosystem through food web
592 modeling. Ecology 93:1707-1716
593 McGuire, A. D., T. R. Christensen, D. Hayes, A. Heroult, E. Euskirchen, J. S. Kimball, C.
594 Koven, P. Lafleur, P. A. Miller, W. Oechel, P. Peylin, M. Williams, and Y. Yi. 2012. An
595 assessment of the carbon balance of arctic tundra: Comparisons among observations,
596 process models, and atmospheric inversions. Biogeosciences 9:3185-3204.
597 McKane, R., E. Rastetter, G. Shaver, K. Nadelhoffer, A. Giblin, J. Laundre, and F. Chapin. 1997.
598 Reconstruction and analysis of historical changes in carbon storage in arctic tundra.
599 Ecology 78:1188-1198.
600 McKinnon, L., P. A. Smith, E. Nol, J. L. Martin, F. I. Doyle, F.I., Abraham, H. G. Gilchrist, R. I.
601 G. Morrison, and J. Bêty. 2010. Lower predation risk for migratory birds at high
602 latitudes. Science 327:326-327
603 McLaren, J. R., and R. L. Jefferies. 2004.. Initiation and maintenance of vegetation mosaics in an
604 Arctic salt marsh. J Ecol 92:648-660.

McNaughton, S. J. 1985. Ecology of a grazing ecosystem: The Serengeti. Ecological Monographs 55:259-294.

Metcalfe, D. B., G. P. Asner, R. E. Martin, J. E. Silva Espejo, W. H. Huasco, F. F. Farfán Amézquita, L. Carranza-Jimenez, D. F. Galiano Cabrera, L.D. Baca, F. Sinca, L. P. Huaraca Quispe, I. A. Taype, L. E. Mora, A. R. Dávila, M. M. Solórzano, B. L. Puma Vilca, J. M. Laupa Román, P. C. Guerra Bustios, N. S. Revilla, R. Tupayachi, C. J. Girardin, C. E. Doughty, and Y. Malhi. 2014. Herbivory makes major contributions to ecosystem carbon and nutrient cycling in tropical forests. Ecology Letters 17:324–32. doi: 10.1111/ele.12233

Metclafe, D. B., and J. Olofsson. 2015. Distinct impacts of different mammalian herbivore assemblages on arctic tundra CO2 exchange during the peak of the growing season. Oikos 124: 1632-1638. https://doi.org/10.1111/oik.02085

Min, E., M. Wilcots, S. Naeem, L. Gough, J. R. McLaren, R. J. Rowe, E. Rastetter, N. Boelman, and K. L. Griffin. 2021. Herbivore absence can shift dry heath tundra from carbon source to sink during peak growing season. Environ. Res. Lett. 162021. 024027

Oli, M. 2019. Population cycles in voles and lemmings: state of the science and future directions. Mammal Review 49 2019. 226–239Roberts, P and Jones DL. 2012. Microbial and plant uptake of free amino sugars in grassland soils. Soil Biology and Biochemistry 49:139-149.

Olofsson, J., H. Tømmervik, and T. V. Callaghan. 2012. Vole and lemming activity observed from space. Nature Climate Change Letters DOI: 10.1038/NCLIMATE1537

Pastor, J. R., J. Naiman, B. Dewey. and P. McInnes. 1988. Moose, microbes and the boreal forest. Bioscience 38:770-779.

628 Pearce, A. R., E. B. Rastetter, W. B. Bowden, M. C. Mack, Y. Jiang, Y., and B. L. Kwiatkowski,
629 B.L. 2015. Recovery of arctic tundra from thermal erosion disturbance is constrained by
630 nutrient accumulation: a modeling analysis. Ecological Applications 25:1271-1289.
631 Petit Bon, M., K. G. Inga, I. S. Jónsdóttir, T. A. Utsi, E. M. Soininen, and K. A. Bråthen. 2020.
632 Interactions between winter and summer herbivory affect spatial and temporal plant
633 nutrient dynamics in tundra grassland communities. Oikos 129:1229-1242.
634 Pitelka, F. A. and G. O. Batzli. 2007. Population cycles of lemmings near Barrow, Alaska: a
635 historical review. Acta Theriologica 52: 323–336.
636 Pitelka, F. A., P. Q. Tomich, and G. W. Treichel. 1955. Ecological relations of jaegers and owls
637 as lemming predators near Barrow, Alaska. Ecological Monographs 25: 85–117.
638 Post, E., and C. Pedersen. 2008. Opposing plant community responses to warming with and
639 without herbivores. Proceedings of the National Academy of Sciences 105, 12353-12358.
640 Prevedello, J. M., C. R. Dickman, M. V. Vieira, and E. M. Vieira, E.M. 2013. Population
641 responses of small mammals to food supply and predators: a global meta-analysis. J
642 Animal Ecol. 82:927-936.
643 Rastetter, EB. 2017. Modeling for understanding v. modeling for numbers. Ecosystems 20:215-
644 221.
645 Rastetter, E. B., G. I. Ågren, and G. R. Shaver. 1997. Responses of N-limited ecosystems to
646 increased CO2: A balanced-nutrition, coupled-element-cycles model. Ecol. Appl. 7: 444–
647 460.
648 Rastetter, E., K. Griffin, R. Rowe, L. Gough, J. McLaren, and N. Boelman. 2021a. ARC-LTER/vole:
649 Initial release - VOLE v4.0 (Version v4.0). Zenodo. http://doi.org/10.5281/zenodo.5083290
650 Rastetter, E., K. Griffin, R. Rowe, L. Gough, J. McLaren, and N. Boelman. 2021b. Modeling the effect of
651 explicit vs implicit representation of grazing on ecosystem carbon and nitrogen cycling in

response to elevated carbon dioxide and warming in arctic tussock tundra, Alaska - Dataset A ver 2. Environmental Data Initiative. https://doi.org/10.6073/pasta/67108cef344d93cfdd060e7e0f0911f5.

Rastetter, E., K. Griffin, R. Rowe, L. Gough, J. McLaren, and N. Boelman. 2021c. Modeling the effect of explicit vs implicit representation of grazing on ecosystem carbon and nitrogen cycling in response to elevated carbon dioxide and warming in arctic tussock tundra, Alaska - Dataset B ver 2. Environmental Data Initiative. https://doi.org/10.6073/pasta/42e6660b2d1f2b59985ed0940e53f0d4.

Rastetter, E. B., G. W. Kling, G. R. Shaver, B. C. Crump, L. Gough, and K. L. Griffin. 2020. Ecosystem recovery from disturbance is constrained by N cycle openness, vegetation-soil N distribution, form of N losses, and the balance between vegetation and soil-microbial processes. Ecosystems https://doi.org/10.1007/s10021-020-00542-3

Rinnan, R., S. Stark, and A. Tolvanen. 2009. Responses of vegetation and soil microbial communities to warming and simulated herbivory in a subarctic heath. Journal of Ecology 97:788–800.

Schmitz, O. J., P. A. Raymond, J. A. Estes, W. A. Kurz, G. W. Holtgrieve, M. E. Ritchie, D. E. Schindler, A. C., Spivak, R. W. Wilson, M. A. Bradford, V. Christensen, L. Deegan, V. Smetacek, M. J. Vanni, and C. C. Wilmers. 2014. Animating the carbon cycle. Ecosystems 17:344-359.

Seagle, S. W. and S. J. McNaughton. 1993. Simulated effects of precipitation and nitrogen on Serengeti grassland productivity. Biogeochemistry, 22,157-178.

Sjögersten, S., R. van der Wal, and S. J. Woodin. 2008.. Habitat type determines herbivory controls over CO2 fluxes in a warmer Arctic. Ecology 89:2103–16.

675 Thornton, P. E., J. F. Lamarque, N. A. Rosenbloom, and N. M. Mahowald. 2007. Influence of
676 carbon-nitrogen cycle coupling on land model response to CO_2 fertilization and climate
677 variability. Global Biogeochemical Cycles 21 GB4018, doi:10.1029/2006GB002868
678 Tissue, D. T., and W. C. Oechell. 1987. Response of *Eriophorum vaginatum* to elevated CO2
679 and temperature in the Alaskan tussock tundra. Ecology 68:401-410.
680 Tuomi, M., S. Stark, K. S. Hoset, M. Väisänen, L. Oksanen, F. J. A. Murguzur, H. Tuomisto, J.
681 Dahlgren, and K. A. Bråthen, K.A. 2019. Herbivore effects on ecosystem process rates in
682 a low-productive system. Ecosystems 22:827-843.
683 Wardle, D. A., R. D. Bardgett, J. N. Klironomos, H. Setälä, W. H., Van der Putten, and D. H.
684 Wall. 2004. Ecological linkages between aboveground and belowground biota. Science
685 304:1629-1633
686 Wilkinson, D. M., and T. N. Sherratt. 2016. Why is the world green? The interactions of top–
687 down and bottom–up processes in terrestrial vegetation ecology, Plant Ecology and
688 Diversity, 9:2, 127-140, DOI: 10.1080/17550874.2016.1178353
689 Yu, Q., H. E. Epstein, D. A. Walker, G. V. Frost, and B. C. Forbes. 2011. Modeling dynamics of
690 tundra plant communities on the Yamal Peninsula, Russia, in response to climate change
691 and grazing pressure. Environmental Research Letters 6. doi:10.1088/1748-
692 9326/6/4/045505.
693 Zimov, N. S., S. A. Zimov, A. E. Zimova, G. H. Zimova, V. I. Chuprynin, and F. S. Chapin III.
694 2009. Carbon storage in permafrost and soils of the mammoth tundra-steppe biome: Role
695 in the global carbon budget. Geophysical Research Letters 36.
696 doi:10.1029/2008GL036332.
697

Box 1: Model Equations. Variables and parameters defined in Table 1.

	MASS-BALANCE EQUATIONS		
1	$\frac{dB_C}{dt} = P_s - L_{itC} - R_a - G_C$	2	$\frac{dB_N}{dt} = U_N - L_{itN} - G_N$
3	$\frac{dD_C}{dt} = L_{itC} + L_{VC} - R_h - Q_{CR}$	4	$\frac{dD_N}{dt} = L_{itN} + U_{Nm} + L_{VN} - N_{min} - Q_{NR}$
		5	$\frac{dN}{dt} = N_{in} + N_{min} + V_{UN} - U_N - U_{Nm} - Q_{DIN}$
	ALLOMETRY & STOICHIOMETRY CONSTRAINTS		
6	$S = B_C \frac{(\propto B_C + 1)}{(\gamma B_C + 1)}$		
7	$\Psi = \frac{B_C}{B_N q_B}$	8	$\Phi = \frac{D_C}{D_N q_D}$
	PROCESS EQUATIONS		
	CARBON		**NITROGEN**
9	$P_s = \frac{g_C S C_a}{\Psi(k_C + C_a)} Q_{10Ps}^{T/10}$	10	$U_N = \frac{g_N \Psi S N}{k_N + N} Q_{10U}^{T/10}$
11	$L_{itC} = m_{CB} B_C$	12	$L_{itN} = \frac{m_{NB}}{\Psi} B_N$

13	$R_{\mathrm{a}}=r_{\mathrm{B}}\,B_{\mathrm{C}}\,\Psi\,Q_{10\mathrm{Ra}}^{T/10}$	14	$U_{\mathrm{Nm}}=\dfrac{g_{\mathrm{Nm}}\,\Phi\,D_{\mathrm{C}}\,N}{k_{\mathrm{Nm}}+N}Q_{10\mathrm{Um}}^{T/10}$
15	$G_{C}=\left(n_{\mathrm{V}}+g_{\mathrm{V}}-\varepsilon_{\mathrm{V}}\left(T-T_{0}\right)\right)V/10000$	16	$G_{\mathrm{N}}=G_{\mathrm{C}}/q_{\mathrm{V}}$
17	$R_{\mathrm{V}}=r_{\mathrm{V}}\left(G_{\mathrm{C}}-n_{\mathrm{V}}\,V/10000\right)$	18	$V_{\mathrm{UN}}=m_{\mathrm{NV}}\,V/10000$
19	$L_{\mathrm{VC}}=G_{\mathrm{C}}-R_{\mathrm{V}}$	20	$L_{\mathrm{VN}}=G_{\mathrm{N}}-V_{\mathrm{UN}}$
21	$R_{\mathrm{h}}=r_{\mathrm{D}}\,D_{\mathrm{C}}\,\Phi\,Q_{10\mathrm{Rh}}^{T/10}$	22	$N_{\min}=\dfrac{m_{\mathrm{Nm}}D_{\mathrm{N}}}{\Phi}\,Q_{10\mathrm{m}}^{T/10}$
23	$Q_{\mathrm{CR}}=q_{\mathrm{DOM}}\,Q_{\mathrm{NR}}$	24	$Q_{\mathrm{NR}}=\beta_{\mathrm{NR}}D_{\mathrm{N}}$
		25	$Q_{\mathrm{DIN}}=\beta_{\mathrm{N}}\,N$

699

700

701

Table 1: Model variables and parameters. Variable values are for the initial steady state with the aggregated representation of vole effects. Ψ and Φ are assumed to equal 1 under this steady state. Q_{10} values are as reported in the main text. Other values are from Pearce et al. (2015) or are fit to analogous functions in Pearce et al. (2015). Parameters are listed to four significant digits.

	Symbol	Value	Units
C and N stocks			
Vegetation C	B_C	878	g C m^{-2}
Detritus and soil organic C	D_C	19452	g C m^{-2}
Vegetation N	B_N	20.6	g N m^{-2}
Detritus and soil organic N	D_N	831	g N m^{-2}
Inorganic N	N	0.27	g N m^{-2}
Processes and constraints			
Allometric constraint	S	243.75	g C m^{-2}
Vegetation stoichiometric constraint	Ψ	1	none
Soil stoichiometric constraint	Φ	1	none
Photosynthesis	P_s	430	g C m^{-2} yr^{-1}
Autotrophic respiration	R_a	215	g C m^{-2} yr^{-1}
Litter-fall C	L_{itC}	215	g C m^{-2} yr^{-1}
Heterotrophic respiration (excluding voles)	R_h	213.07	g C m^{-2} yr^{-1}
Vegetation N uptake	U_N	5.3800	g N m^{-2} yr^{-1}
Litter-fall N	L_{itN}	5.3800	g N m^{-2} yr^{-1}
Gross N mineralization	N_{min}	19.7310	g N m^{-2} yr^{-1}
N immobilization	U_{Nm}	14.4824	g N m^{-2} yr^{-1}
Inorganic N losses	Q_{DIN}	0.0016	g N m^{-2} yr^{-1}

Refractory N losses	Q_{NR}	0.1314	g N m^{-2} yr^{-1}
Refractory C losses	Q_{CR}	1.93	g C m^{-2} yr^{-1}
C removed from vegetation by voles	G_C	0	g C m^{-2} yr^{-1}
Vole respiration	R_V	0	g C m^{-2} yr^{-1}
C added to soil organic matter by voles	L_{VC}	0	g C m^{-2} yr^{-1}
N removed from vegetation by voles	G_N	0	g N m^{-2} yr^{-1}
C added to soil organic matter by voles	L_{VN}	0	g N m^{-2} yr^{-1}
Vole N transfer vegetation to inorganic soil	V_{UN}	0	g N m^{-2} yr^{-1}
Driver variables			
Atmospheric CO2	C_a	400	μmol mol^{-1}
Temperature	T	10	ºC
N inputs	N_{in}	0.1330	g N m^{-2} yr^{-1}
Voles	V	0	voles ha^{-1}
Parameters			
Allometric parameter 1	α	0.002231	m^2 g^{-1} C
Allometric parameter 2	γ	0.01100	m^2 g^{-1} C
Optimum vegetation C:N	q_B	42.62	g C g^{-1} N
Optimum soil C:N	q_D	23.41	g C g^{-1} N
Photosynthesis rate parameter	g_C	1.423	yr^{-1}
CO_2 half-saturation constant	k_C	100.0	μmol mol^{-1}
Photosynthesis Q-10	Q_{10Ps}	1.550	none
Autotrophic respiration constant	r_B	0.09069	yr^{-1}
Autotrophic respiration Q-10	Q_{10Ra}	2.700	none
Vegetation C turnover rate constant	m_{CB}	0.2449	yr^{-1}

Vegetation N-uptake rate parameter	g_N	0.05191	g N g^{-1} C yr^{-1}
Vegetation N half-saturation constant	k_N	1.000	g N m^{-2}
Vegetation N-uptake Q-10	Q_{10U}	2.000	none
Vegetation N turnover rate constant	m_{NB}	0.2612	yr^{-1}
Heterotrophic respiration constant	r_D	0.003651	yr^{-1}
Heterotrophic respiration Q-10	Q_{10Rh}	3.000	none
Microbial N-uptake rate parameter	g_{Nm}	0.001796	g N g^{-1} C yr^{-1}
Microbial N half-saturation constant	k_{Nm}	1.000	g N m^{-2}
Microbial N-uptake Q-10	Q_{10Um}	1.950	none
Vole nesting material	n_V	22	g C $vole^{-1}$ yr^{-1}
Vole C ingestion rate	g_V	3512	g C $vole^{-1}$ yr^{-1}
Temperature slope vole metabolism	ε_V	52	g C $vole^{-1}$ $^oC^{-1}$ yr^{-1}
Summer to annual temperature correction	T_0	10	^oC
C:N of vole forage and nest material	q_V	19.15	g C g^{-1} N
Vole base respiration rate	r_V	0.3	none
Vole urine N production rate	m_{NV}	11.00	g N $vole^{-1}$ yr^{-1}
Soil organic N turnover constant	m_{Nm}	0.01099	yr^{-1}
Soil organic N turnover Q-10	Q_{10m}	2.160	none
C:N of DOM loss	q_{DOM}	14.69	g C g^{-1}N
N loss-rate parameter	β_N	0.005926	yr^{-1}
Refractory N loss parameter	β_{NR}	0.0001581	yr^{-1}

706

707

Table 2: Variable and parameter changes to accommodate the effect of explicit representation of voles. Values in parentheses are the percent change from the values used in the implicit-vole representation with vole effects aggregated in with parallel ecosystem processes. "Total" is the total of the vole-mediated and the parallel ecosystem process in the two preceding rows. "PAR" is the parameter in the equation for the parallel process in the preceding rows that was modified to accommodate explicit representation of voles.

	Symbol	vole effects aggregated in with other processes	explicit vole representation with 40 voles ha^{-1}	explicit vole representation with 100 voles ha^{-1}	units
	L_{itC}	215	200.864 (-6.6%)	179.66 (-16.4%)	g C m^{-2} yr^{-1}
	G_C	0	14.136	35.34	g C m^{-2} yr^{-1}
Total		215	215	215	g C m^{-2} yr^{-1}
PAR	m_{CB}	0.2449	0.2288 (-6.6%)	0.2046 (-16.4%)	yr^{-1}
	R_h	213.07	208.8556 (-2.0%)	202.534 (-4.9%)	g C m^{-2} yr^{-1}
	R_v	0	4.2144	10.536	g C m^{-2} yr^{-1}
Total		213.07	213.07	213.07	g C m^{-2} yr^{-1}
PAR	r_D	0.003651	0.003658 (-2.0%)	0.003471 (-4.9%)	yr^{-1}
	L_{itN}	5.38	4.6418 (-13.7%)	3.5346 (-34.3%)	g N m^{-2} yr^{-1}

	G_N	0	0.7382	1.8454	g N m^{-2} yr^{-1}
Total		5.38	5.38	5.38	g N m^{-2} yr^{-1}
PAR	m_{NB}	0.2612	0.2253 (-13.7%)	0.1716 (-34.3%)	yr^{-1}
	V_{UN}	0	0.044	0.110	g N m^{-2} yr^{-1}
	N_{min}	19.731	19.687 (-0.2%)	19.621 (-0.6%)	g N m^{-2} yr^{-1}
Total		19.731	19.731	19.731	g N m^{-2} yr^{-1}
PAR	m_{Nm}	0.01099	0.01097 (-0.2%)	0.01093 (-0.6%)	yr^{-1}

714

715

716 **Table 3:** Calibrations

Calibration	Vole representation	Vole density
I	vole effects aggregated in with other processes	Unspecified vole density, but vole effects subsumed into litter fall C and N, heterotrophic respiration, and N mineralization in the calibration (Table 2).
II	explicit vole representation	40 voles ha^{-1}
III	explicit vole representation	100 voles ha^{-1}

717

718

719 **Table 4**: Simulations

Simu-lation	Cali-bration	Description	Figure
Set 1:			
1	**II**	constant 40 voles ha^{-1}	Fig. 2 dotted black lines
2	**II**	voles cycling as in Fig. 1	Fig. 2 cycling black solid lines
3	**II**	voles cycling as in Fig. 1 for 10 years then held constant at 100 voles ha^{-1}	Fig. 2 dashed red lines
4	**II**	voles cycling as in Fig. 1 for 10 years then held constant at 0 voles ha^{-1}	Fig. 2 dash-dotted blue lines
Set 2:			
5	**I**	vole density unspecified, linear increase of CO_2 from 400 to 800 μmol mol^{-1}over 100 years	Figs. 4, 5, & 6 dotted line, left column
6	**I**	vole density unspecified, linear increase in temperature from 10 to 15 ºC over 100 years	Figs. 4, 5, & 6 dotted line, middle column
7	**I**	vole density unspecified, linear increase of CO_2 from 400 to 800 μmol mol^{-1} and temperature from 10 to 15 ºC over 100 years	Figs. 4, 5, & 6 dotted line, right column
8	**II**	vole density cycling as in Fig. 1, linear increase of CO_2 from 400 to 800 μmol mol^{-1}over 100 years	Figs. 4, 5, & 6 blue solid line, left column

9	**II**	vole density cycling as in Fig. 1, linear increase in temperature from 10 to 15 ºC over 100 years	Figs. 4, 5, & 6 blue solid line, middle column
10	**II**	vole density cycling as in Fig. 1, linear increase of CO_2 from 400 to 800 μmol mol^{-1} and temperature from 10 to 15 ºC over 100 years	Figs. 4, 5, & 6 blue solid line, right column
11	**III**	constant 100 voles ha^{-1}, linear increase of CO_2 from 400 to 800 μmol mol^{-1}over 100 years	Figs. 4, 5, & 6 dashed red line, left column
12	**III**	constant 100 voles ha^{-1}, linear increase in temperature from 10 to 15 ºC over 100 years	Figs. 4, 5, & 6 dashed red line, middle column
13	**III**	constant 100 voles ha^{-1}, linear increase of CO_2 from 400 to 800 μmol mol^{-1} and temperature from 10 to 15 ºC over 100 years	Figs. 4, 5, & 6 dashed red line, right column

720

721

FIGURE CAPTIONS

Figure 1: Vole cycle used to simulate ecosystem response to grazing. Vole abundance is randomly generated with peaks every three or four years, with abundances at the peak ranging from 90 to 110 voles ha^{-1}, minimum abundances ranging from 8 to 12 voles ha^{-1}, and a mean vole abundance of 40 voles ha^{-1}. Upper panel shows the first 30 years of the time series. Bottom panel is the full 200-year time series.

Figure 2: Simulated changes in plant and soil organic carbon (C) and nitrogen (N) in response to constant vole abundance, vole cycling, vole density maintained at 100 voles ha^{-1}, and vole removal (see Table 4). The thin dotted black lines are the steady state values if vole density is held at 40 voles ha^{-1} (simulation 1). Solid black lines are the responses to the vole cycle depicted in figure 1 (simulation 2). Dashed red lines are the responses to the same vole cycle and then vole density maintained at 100 voles ha^{-1} after year 10 (simulation 3). Dashed-dotted blue lines are the responses to the same vole cycle and then removal of voles after year 10 (simulation 4).

Figure 3: Plant carbon (C) and nitrogen (N) recovery following peak vole abundance in simulation 2. The plant C and N of 875 g C m^{-2} and 20.2 g N m^{-2} were selected to partition the recovery time series into two approximately equal-sized groups based on their values at the time of the previous vole peak (time 0 on x axis). The levels of C and N during this recovery depend not only on peak vole abundance, but also on the degree of recovery following the previous vole cycle. Because the biomass consumed is proportional to vole abundance and not to plant biomass, if plants recover to a higher level following the previous cycle (white dots), then they

745 begin and maintain recovery in the current cycle at a higher level relative to plants that recovered
746 to a lower level in the previous cycle (black dots). This autocorrelation results in the longer-term
747 dynamics in Fig. 2 for simulation 2 in which vole abundance cycled. The recovery in any cycle
748 also depends on vole abundance and the duration of the vole cycle (higher plant recovery in a 4-
749 year cycle than a 3-year cycle).
750
751 **Figure 4:** Simulated changes in plant, soil, and total ecosystem C with a linear increase in CO_2
752 from 400 to 800 μmol mol^{-1} over 100 years, a linear warming from 10 to 15 ºC over 100 years,
753 and both a linear increase in CO_2 from 400 to 800 μmol mol^{-1} and a linear warming from 10 to
754 15 ºC over 100 years (see Table 4). Different trajectories indicate responses with vole effects
755 aggregated with other biogeochemical processes (dotted black lines; simulations 5, 6, & 7), voles
756 cycling between 8 and 110 voles ha^{-1} on a three-to-four-year cycle (solid blue lines; simulations
757 8, 9, & 10), and a constant 100 voles ha^{-1} (dashed red lines; simulations 11, 12, & 13).
758
759 **Figure 5**: Simulated changes in plant, soil, and total ecosystem N with a linear increase in CO_2
760 from 400 to 800 μmol mol^{-1} over 100 years, a linear warming from 10 to 15 ºC over 100 years,
761 and both a linear increase in CO_2 from 400 to 800 μmol mol^{-1} and a linear warming from 10 to
762 15 ºC over 100 years (see Table 4). Different trajectories indicate responses with vole effects
763 aggregated with other biogeochemical processes (dotted black lines; simulations 5, 6, & 7), voles
764 cycling between 8 and 110 voles ha^{-1} on a three-to-four-year cycle (solid blue lines; simulations
765 8, 9, & 10), and a constant 100 voles ha^{-1} (dashed red lines; simulations 11, 12, & 13).
766

Figure 6: Simulated changes in gross primary (GPP), net primary (NPP), and net ecosystem production (NEP) with a linear increase in CO_2 from 400 to 800 μmol mol^{-1} over 100 years, a linear warming from 10 to 15 ºC over 100 years, and both a linear increase in CO_2 from 400 to 800 μmol mol^{-1} and a linear warming from 10 to 15 ºC over 100 years (see Table 4). Different trajectories indicate responses with vole effects aggregated with other biogeochemical processes (dotted black lines; simulations 5, 6, & 7), voles cycling between 8 and 110 voles ha^{-1} on a three-to-four-year cycle (solid blue lines; simulations 8, 9, & 10), and a constant 100 voles ha^{-1} (dashed red lines; simulations 11, 12, & 13).

Figure 7: Causal-chain diagram for the model in Box 1. Arrows indicate causal links: a red arrow marked with a "+" indicates that an increase in the variable at the tail of the arrow will cause an increase in the variable at the head of the arrow; a blue arrow marked with a "-" indicates that and increase in the variable at the tail of the arrow will cause a decrease in the variable at the head of the arrow. Symbols are defined in Table 1. Symbols in boxes are C and N stocks, symbols in circles are driver variables, and other symbols are either processes or allometric and stoichiometric constraints. The four causal links shown as dashed arrows are the links that were weakened in the calibration to accommodate vole-mediated processes in the simulations with explicit representation of vole density (see Table 2). The temperature (*T*) and vole (*V*) drivers are shown three times to avoid over complicating the diagram.

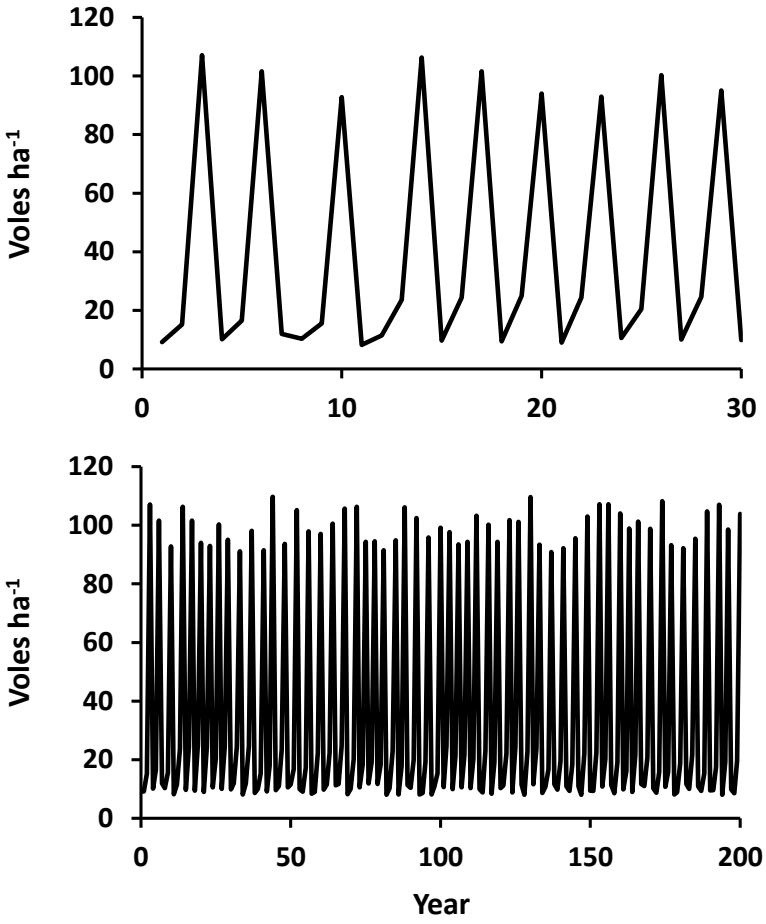
120
100
80
60
40
20
0
Voles ha-1
0
10
20
30
120
100
80
60
40
20
0
Voles ha-1
0
50
100
150
200
Year

Fig. 1

787

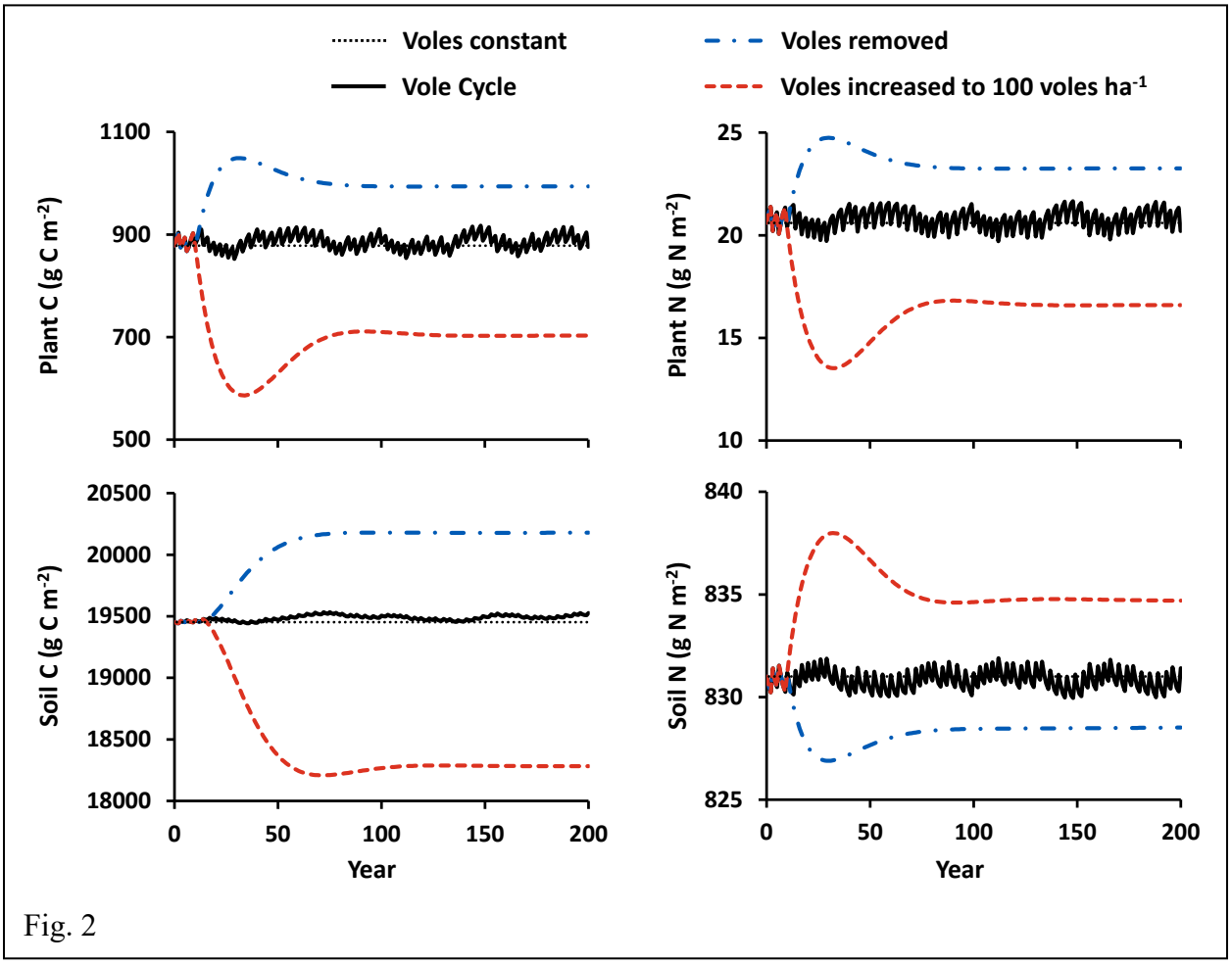
Voles constant
Vole Cycle
Voles removed
Voles increased to 100 voles ha-1
Plant C (g C m-2)
Plant N (g N m-2)
Soil C (g C m-2)
Soil N (g N m-2)
Year
Year

Fig. 2

788
789

790

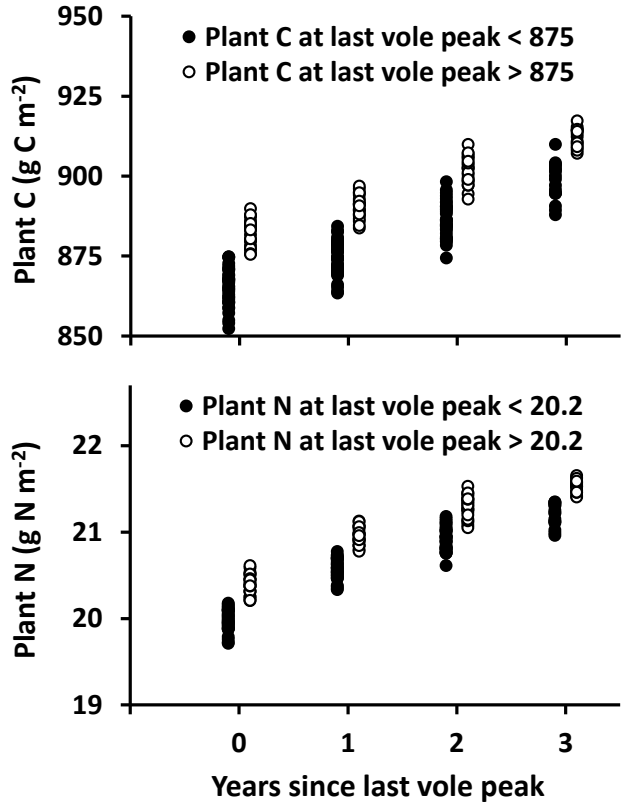

Fig. 3

791

792

793

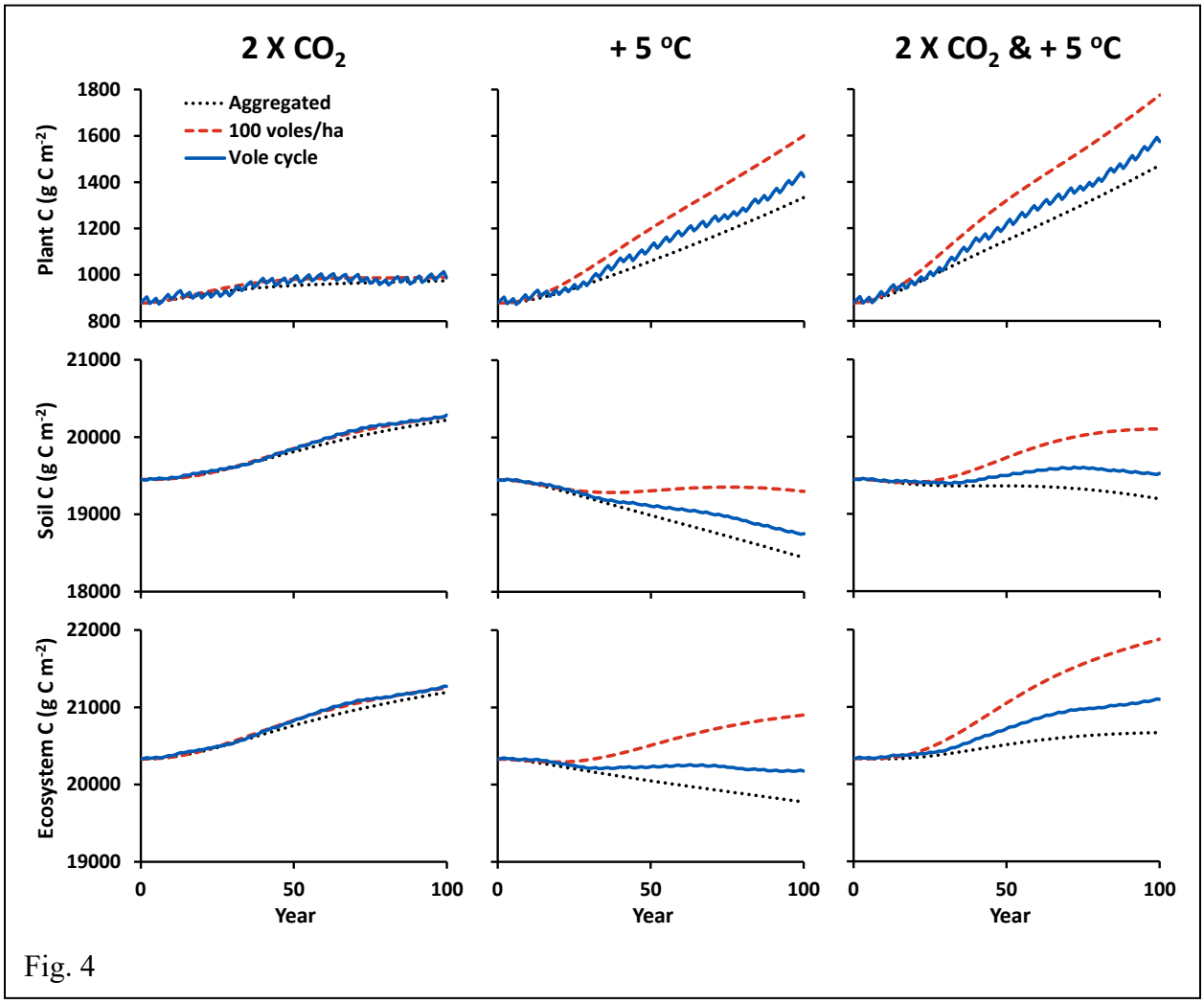

Fig. 4

794
795

796
797

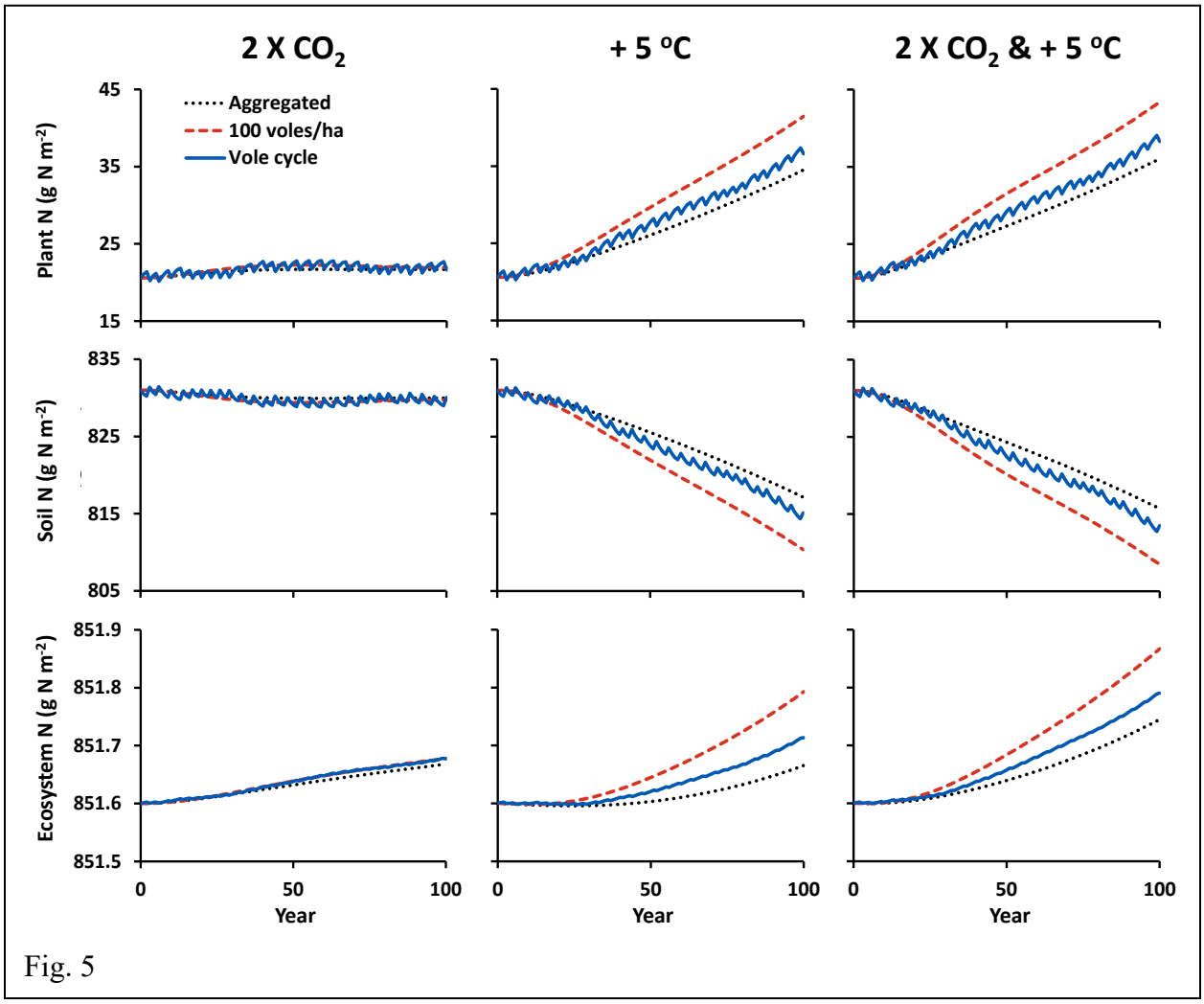

Fig. 5

798
799

800
801

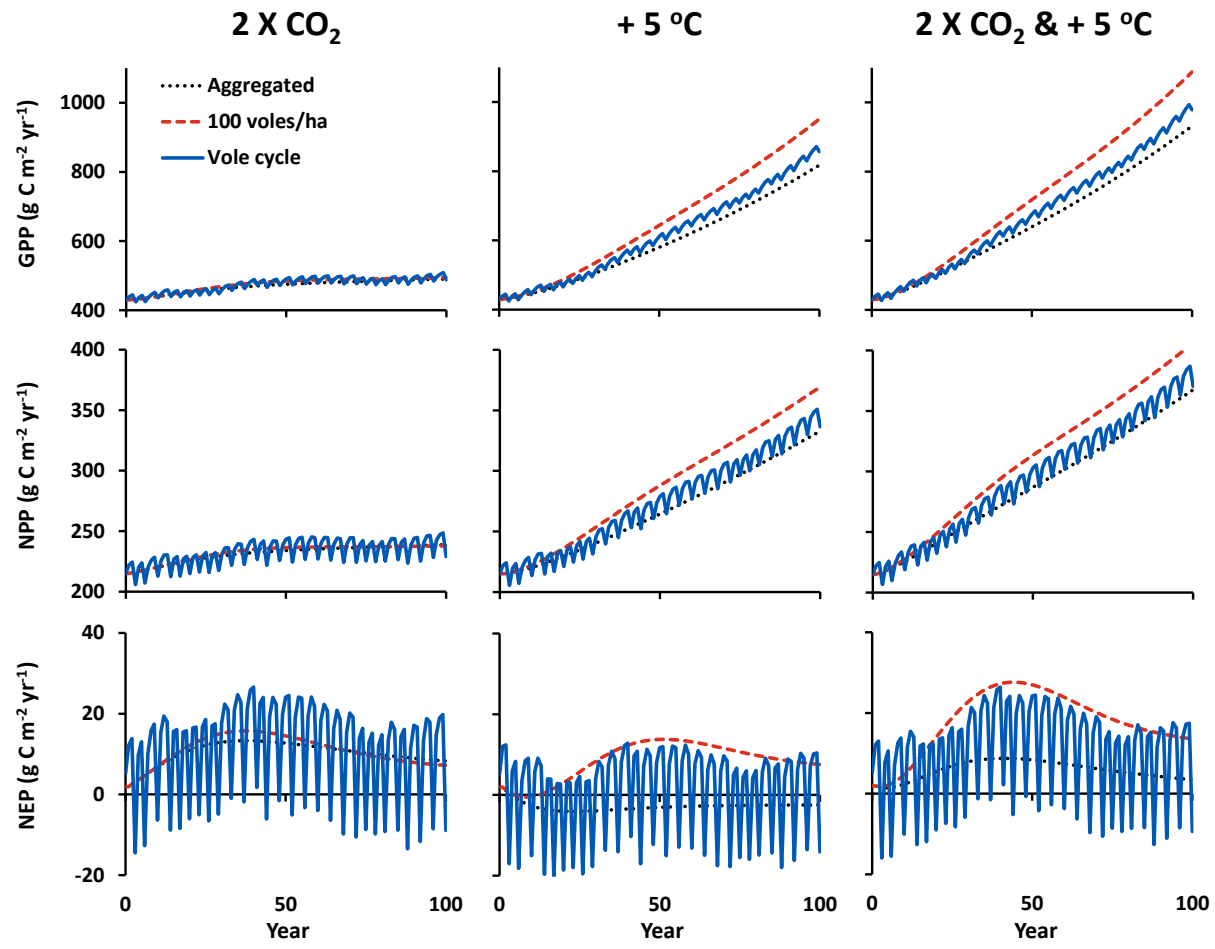

Fig. 6

802
803

804
805

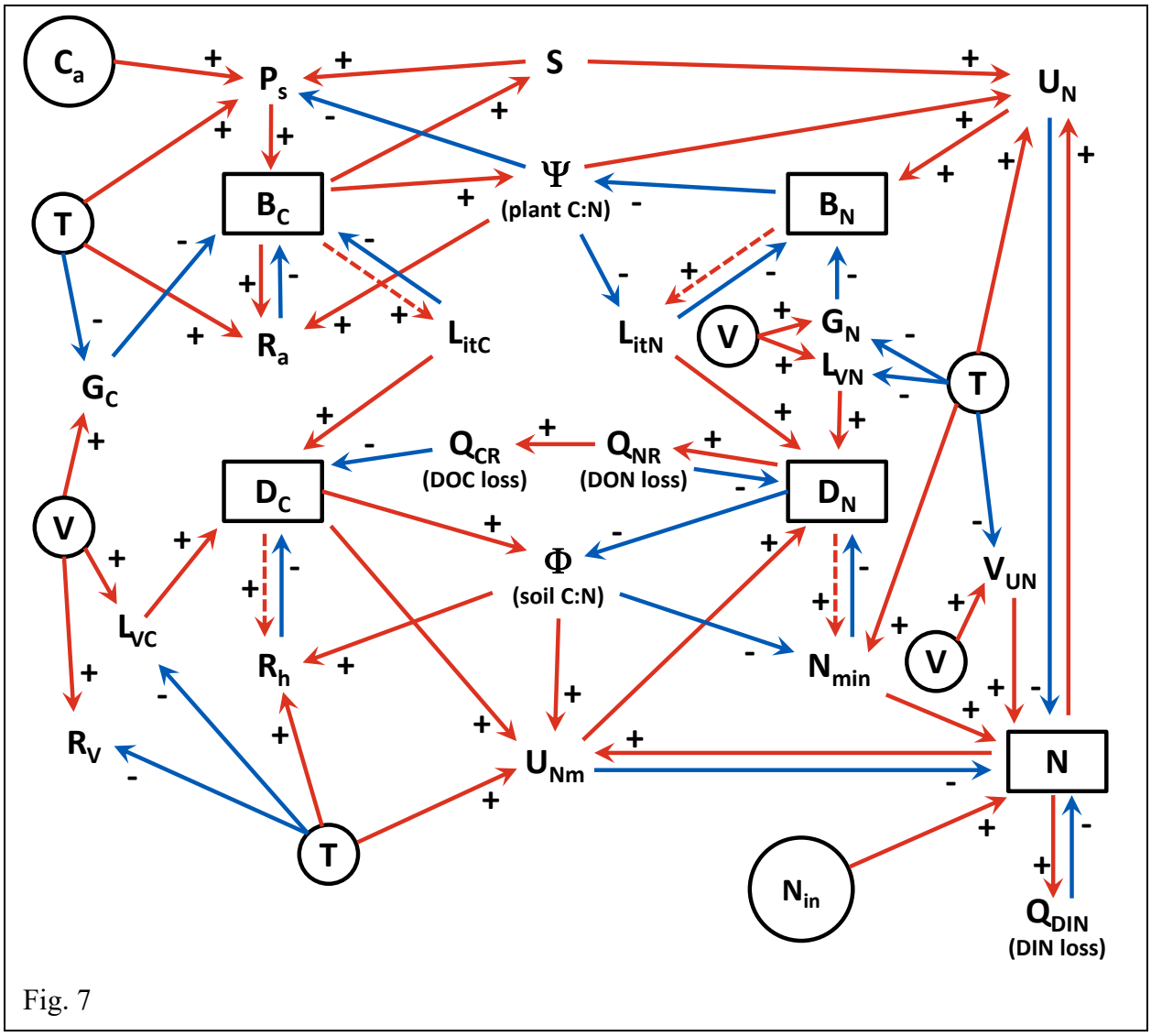

Fig. 7

806
807
808

Appendix S1: Derivation of stocks, fluxes and parameter values.

Section S1: Calibration for the aggregated model (vole activity not explicitly represented)

We set C and N stocks and fluxes to be consistent with data collated by Pearce et al. (2015) for the Multiple Element Limitation (MEL) model applied to tussock tundra (Table 2 in main text). Our detritus C and N are the aggregated value of the three detritus stocks the MEL model. To compensate for differences in model structures, we calculated litter-fall C and N (L_{itC} and L_{itN}), heterotrophic respiration (R_h), N immobilization (U_{Nm}), and N inputs (N_{in}) by difference assuming the ecosystem was in steady state.

We derived parameter values from various sources. We fit our allometric parameters (α and γ) to the MEL allometric equation for tundra from Pearce et al. (2015). We assume a stoichiometric balance for calibration and therefore set the optimum vegetation and detritus C:N ratios (q_B and q_D) to the C:N ratios of the respective stocks from Pearce et al. (2015). Similarly, we set the C:N of dissolved organic matter losses (q_{DOM}) to the ratio of the respective fluxes estimated from Pearce et al. (2015). To mimic the CO_2 response reported in Tissue and Oechell (1987), we set the CO_2 half-saturation constant for photosynthesis (k_C) to 100 μmol mol^{-1}. To impose strong N limitation (Shaver et al. 2014), we set both the half saturation constants for plant (k_N) and microbial (k_{Nm}) N uptake to 1 g N m^{-2} as in Rastetter et al. (2020).

We also set the temperature responses based on data from various sources. For photosynthesis we use a Q_{10} value of 1.55, which is a median of values derived from data in Tieszen (1973) and Rogers et al. (2019). For autotrophic respiration we use a Q_{10} of 2.7 based on a fit between 10 and 15 ºC to the model for tundra species in Heskel et al. (2016). For heterotrophic respiration we use a Q_{10} of 3 again based on a fit between 10 and 15 ºC to the

832 model for Boreal forest soils in Carey et al. (2016). Atkin and Cummins (1994) report ^{15}N-based
833 uptake rates for arctic plants consistent with Q_{10} values ranging from 1.16 to 3.17. Dong et al.
834 (2001) and Yan et al. (2012) report plant N uptake rates in an agricultural setting consistent with
835 Q_{10} values of 3.99 and 1.67. Based on these studies, we assume a Q_{10} of 2 for N uptake by
836 plants. For microbial N uptake (immobilization), we use a Q_{10} value of 1.95 as reported by
837 Roberts and Jones (2012) for microbial uptake of amino sugars. Finally, for N mineralization,
838 Roberts and Jones (2012) report a Q_{10} value of 2.32 and Vinolas et al. (2001) report a value of 2;
839 we use a Q_{10} value of 2.16.
840 Except for parameters associated with vole activity, the only parameters remaining are
841 the rate parameters for each of the C and N fluxes. We calibrate these rate parameters to the
842 process rates reported in Pearce et al. (2015) for the MEL model applied to tussock tundra (Table
843 2 in main text).
844
845 **Section S2:Calibration of the distributed model (explicit representation of vole activity)**
846 We assume generic small mammals (voles and lemmings) weighing 50 g, but will refer to
847 them as a "voles." We estimate C removal from vegetation by voles from two processes,
848 consumption and nest building. The consumption rates depend on an allometric relation to body
849 weight minus a correction for temperature to compensate for the energy needed to maintain body
850 temperature (Batzli et al. 1980). We modify this function to account for the difference between
851 the summer temperature we use to drive the model and subnivean temperature during the winter.
852 We assume that the average annual temperature experienced by the voles is ten degrees cooler
853 than the average summer temperature:
854

$$E = 26.82 + 5.36\,W^{0.75} - 1.89\,(T - 10)$$

where E is daily energy expenditure (kJ/vole/day), W is body weight (g fresh weight/vole), T is mean summer temperature (°C). For a 50 g vole, this equation simplifies to

$$E = 127.6 - 1.89\,(T - 10)$$

Total food assimilation must meet this energy expenditure, but only about 33% of ingested forage gets assimilated (Batzli et al. 1980). Thus, total ingestion must contain about three times this amount of energy. To convert this ingestion to g C vole^{-1} yr^{-1}, we assume a forage energy density of 18.9 kJ/g dry weight (Batzli et al. 1980) and a C density of forage of 0.475 g C/g dry weight (Schlesinger 1991):

$$I = 3512 - 52\,(T - 10)$$

where I is ingestion (g C vole^{-1} yr^{-1}). Thus, for the ingestion part of Eq. 15 (Table 1 in main text)

$g_V = 3512$ g C vole^{-1} yr^{-1}, $\varepsilon_V = 52$ g C °C^{-1} vole^{-1} yr^{-1}, and $T_0 = 10$ °C

Voles and lemmings also remove plant material to build winter nests. Vole nests contain about 20 g C nest^{-1} (Rowe unpub. data). Krebs et al. (2012) estimate approximately 2.2 nests per lemming in the spring. Data from Maguire and Rowe (2017) indicate that singing vole density in spring is about half the average annual density. We therefore estimate that in addition to

878 ingestion, our generic small mammal (vole) grazer removes 22 g C vole^{-1} yr^{-1} from the vegetation
879 for nests. We add this nest C to the ingestion equation to get the final parameter for Eq. 15:
880
881 $$n_V = 22 \text{ g C vole}^{-1} \text{ yr}^{-1}$$
882
883 Respiration is about 30% of ingestion (Batzli et al. 1980):
884
885 $$r_V = 0.3 \text{ g C g}^{-1} \text{ C}$$
886
887 Forage contains about 25 mg N/g dry weight (Batzli et al. 1980), which is equivalent to a
888 C:N ratio of 19 g C g^{-1} N. We assume the C:N ratio of the nest material is the same as that of
889 the vegetation (42.62 g C/g N). We calculate the C:N of material removed from vegetation by
890 voles as the weighted mean of these two C:N ratios:
891
892 $$q_V = \frac{3512 \times 19 + 22 \times 42.62}{3534} = 19.15 \text{ g C g}^{-1} \text{ N}$$
893
894 We set the per capita urine N production based on data for small mammals reported by Clark et
895 al. (2005):
896
897 $$m_{NV} = 11 \text{ g N vole}^{-1} \text{ yr}^{-1}$$
898
899
900 **Section S3: LITERATURE CITED**

Atkin, O. K., and W. R. Cummins. 1994. The effect of root temperature on the induction of nitrate reductase activities and nitrogen uptake rates in arctic plant species. Plant ans Soil 159:187-197.

Batzli, G. O., R. G. White, S. F. MacLean Jr, F. A. Pitelka, and B. D. Collier. 1980. The herbivore-based trophic system. pp 335-410 in Brown, J., Miller, P.C., Tieszen, L.L., and Brunnell, F.L. eds.. An Arctic Ecosystem: the Coastal Tundra at Barrow, Alaska. Dowden, Hutchinson, and Ross Inc, Stroudsburg, PA, USA

Carey, J. C., J. Tang, P. H. Templar, K. D. Kroger, T. W. Crowther, A. J. Burton, J. S. Dukes, B. Emmett, S. D. Frey, M. A. Heskel, L. Jiang, M. B. Machmuller, J. Mohan, A. M. Panetta, P. B. Reich, S. Reinsch, X. Wang, S. D. Allison, C. Bamminger, S. Bridgham, S. L. Collins, G. de Dato, W. C. Eddy, B. J. Enquist, M. Estiarte, J. Harte, A. Henderson, B. R. Johnson, K. S. Larsen, Y. Luo, S. Marhan, J. M. Melillo, J. Peñuelas, L. Pfeifer-Meister, C. Poll, E. Rastetter, A. B. Reinmann, L. L. Reynolds, I. K. Schmidt, G. R. Shaver, A. L. Strong, V. Suseela, and A. Tietema. 2016. Temperature response of soil respiration largely unaltered with experimental warming. Proc Nat Accad Sci 113:13797-13802.

Clark, J. E., E. C. Hellgren, J. L. Parsons, E. E. Jorgensen, D. M. Engle, and D. M. Lesli Jr. 2005. Nitrogen outputs from fecal and urine deposition of small mammals: implications for nitrogen cycling. Oecologia 144:447-455.

Dong, S., C. F. Scagel, L. Cheng, L. H. Fuchigami, and P. T. Rygiewicz. 2001. Soil temperature and plant growth stage influence nitrogen uptake and amino acid concentration of apple during early spring growth. Tree Phys. 21:541-547.

923 Heskel, M. A., O. S. O'Sullivan, P. B. Reich, M. G. Tjoelker, L. K. Weerasinghe, A. Penillard, J.
924 J. G. Egerton, D. Creek, K. J. Bloomfield, J. Xiang, F. Sinca, Z. R. Stangl, A. Martinez-
925 de la Torre, K. L. Greffin, C. Huntingford, V. Hurry, P. Meir, M. H. Turnbull, and O. K.
926 Atkin. 2016. Convergence in the temperature response of leaf respiration across biomes
927 and plant functional types. Proc Nat Accad Sci 113: 3832-3837.
928 Krebs, C. J., F. Bilodeau, D. Reid, G. Gauthier, A. J. Kenney, S. Gilbert, D. Duchesne, and D. J.
929 Wilson. 2012. Are lemming winter nest counts a good index of population density? J
930 Mammalogy 93:87-92.
931 Maguire, A. J., and R. J. Rowe. 2017. Home range and habitat affinity of the singing vole on the
932 North Slope of Alaska. Arctic, Antarctic, and Alpine Research 492.:243–257.
933 Pearce, A. R., E. B. Rastetter, W. B. Bowden, M. C. Mack, Y. Jiang, Y., and B. L. Kwiatkowski,
934 B.L. 2015. Recovery of arctic tundra from thermal erosion disturbance is constrained by
935 nutrient accumulation: a modeling analysis. Ecological Applications 25:1271-1289.
936 Rastetter, E. B., G. W. Kling, G. R. Shaver, B. C. Crump, L. Gough, and K. L. Griffin. 2020.
937 Ecosystem recovery from disturbance is constrained by N cycle openness, vegetation-soil
938 N distribution, form of N losses, and the balance between vegetation and soil-microbial
939 processes. Ecosystems https://doi.org/10.1007/s10021-020-00542-3
940 Roberts. P., and D. L. Jones. 2012. Microbial and plant uptake of free amino sugars in grassland
941 soil. Soil Biology Biochemistry 49:139-149.
942 Rogers, A., S. P. Serbin, K. S. Ely, and S. D. Wullschleger. 2019. Terrestrial biosphere models
943 may overestimate arctic CO_2 assimilation if they do not account for decreased quantum
944 yield and convexity at low temperature. New Phytologist 223:167-179.

945 Schlesinger, W. H. 1991. Biogeochemistry: An Analysis of Global Change. Academic Press, San
946 Diego, CA, USA.
947 Shaver, G. R., J. A. Laundre, M. S. Bret-Harte, F. S. Chapin, III, J. A. Mercado- Diaz, A. E.
948 Giblin, L. Gough, W. A. Gould, S. E. Hobbie, G. W. Kling, M. C. Mack, J. C. Moore, K.
949 J. Nadelhoffer, E. B. Rastetter, and J. P. Schimel, J.P. 2014. Terrestrial Ecosystems at
950 Toolik Lake, Alaska. In Hobbie, J.E., and G. W. Kling (eds.). A Changing Arctic:
951 Ecological Consequences for Tundra, Streams and Lakes. Oxford University Press, New
952 York, NY, USA.
953 Tieszen, L. L. 1973. Photosynthesis and respiration in arctic tundra grasses: field light intensity
954 and temperature responses. Arctic Alpine Res 5:239-251.
955 Tissue, D. T., and W. C. Oechell. 1987. Response of *Eriophorum vaginatum* to elevated CO2
956 and temperature in the Alaskan tussock tundra. Ecology 68:401-410.
957 Vinolas, L. C., V. R. Vallejo, and D. L. Jones. 2001. Control of aminoacid mineralization and
958 microbial metabolism by temperature. Soil Biology Biochemistry 33:1137-1140.
959 Yan, Q., Z. Duan, J. Mao, X. Li, and F. Dong. 2012. Effects of root-zone temperature and N, P,
960 and K supplies on nutrient uptake of cucumber *Cucumis sativus L.*. seedlings in
961 hydroponics. Soil Science and Pland Nutrition 58:707-717.
962
963